Oocyte spindle assembly depends on multiple interactions between HP1 and the CPC

Lin-Ing Wang[1] , Tyler DeFosse, Janet K. Jang, Rachel A. Battaglia[2], Victoria F. Wagner and Kim S. McKim

Waksman Institute and Department of Genetics, Rutgers, the State University of New Jersey, Piscataway N.J. 08854-8020

Running title: Acentrosomal spindle assembly in oocytes

Key Words: meiosis, chromosome segregation, kinetochore, oocyte, chromosome passenger complex, central spindle

Corresponding author: Kim S. McKim

Waksman Institute, Rutgers University

190 Frelinghuysen Rd

Piscataway, NJ 08854

(848) 445 1164

mckim@waksman.rutgers.edu

[1] Current Address: Mortimer B. Zuckerman Mind Brain and Behavior Institute, 3227 Broadway, 9th Floor-L9-008, New York, NY 10027

[2] 5332 MBRB, Campus box 7545, 111 Mason Farm Rd, Chapel Hill, NC 27599

Abstract

The chromosomes in the oocytes of many animals appear to promote bipolar spindle assembly. In *Drosophila* oocytes, spindle assembly requires the chromosome passenger complex (CPC), which consists of INCENP, Borealin, Survivin and Aurora B. To determine what recruits the CPC to the chromosomes and its role in spindle assembly, we developed a strategy to manipulate the function and localization of INCENP, which is critical for recruiting the Aurora B kinase. We found that an interaction between Borealin and the chromatin is crucial for the recruitment of the CPC to the chromosomes and is sufficient to build kinetochores and recruit spindle microtubules. We also found that HP1 moves from the chromosomes to the spindle microtubules along with the CPC. We propose that the interaction with HP1 promotes the movement of the CPC from the chromosomes to the microtubules. In addition, within the central spindle, rather than at the centromeres, the CPC and HP1 are required for homologous chromosome bi-orientation.

37 # Introduction

38 Accurate chromosome segregation during cell division requires bi-orientation of
39 homologous chromosomes in meiosis I and sister chromatids in mitosis or meiosis II. Bi-
40 orientation is the result of two simultaneous processes: the assembly of microtubules into a
41 bipolar spindle and the correct attachment of the kinetochores to microtubules. In mitosis and
42 male meiosis, the bipolarity of the spindle is defined by centrosomes at each pole. These serve as
43 microtubule organizing centers, nucleating microtubules that grow towards the chromosomes
44 and make contact with kinetochores (Cheeseman, 2014; Heald and Khodjakov, 2015; Nicklas,
45 1997; Watanabe, 2012). In the oocytes of many species, the female meiotic spindle assembles
46 without centrosomes. Spindly assembly initiates when microtubules cluster around the
47 chromosomes after nuclear envelope breakdown (Dumont and Desai, 2012; Radford et al.,
48 2017). In mouse oocytes, this involves the accumulation of acentriolar MTOCs around the
49 chromosomes (Schuh and Ellenberg, 2007). In contrast, the chromosomes or chromatin serve as
50 the sites of microtubule nucleation in the oocytes of *Drosophila* (Matthies et al., 1996; Theurkauf
51 and Hawley, 1992), *Xenopus* (Heald et al., 1996) and human (Holubcová et al., 2015).

52 Chromatin-coated beads in *Xenopus* extracts (Heald et al., 1996; Sampath et al., 2004)
53 and chromosomes without kinetochores in *Drosophila* oocytes (Radford et al., 2015) build
54 spindles. Similarly, kinetochore-independent chromosome interactions between the
55 chromosomes and the spindle in *C. elegans* oocyte meiosis have been observed (Dumont et al.,
56 2010; Muscat et al., 2015; Wignall and Villeneuve, 2009). These results suggest that oocyte
57 chromatin carries signals that can recruit and organize spindle assembly factors. Potential targets
58 of these signals include the Ran pathway and the Chromosomal Passenger Complex (CPC), both
59 of which have been shown to promote chromosome-directed spindle assembly (Bennabi et al.,
60 2016; Drutovic et al., 2020; Mullen et al., 2019; Radford et al., 2017). The CPC comprises

61 Aurora B kinase, the scaffold subunit INCENP, and the two targeting subunits Borealin and
62 Survivin (Deterin in *Drosophila*). In *Drosophila*, the depletion of Aurora B or INCENP causes a
63 complete failure of meiotic spindle assembly in oocytes (Colombié et al., 2008; Radford et al.,
64 2012). Similarly, the CPC is required for promoting spindle assembly when sperm nuclei are
65 added to *Xenopus* egg extracts (Kelly et al., 2007; Maresca et al., 2009; Sampath et al., 2004).
66 The results in *Xenopus* and *Drosophila* suggest that oocyte chromosomes carry signals that can
67 recruit and activate the activity of the CPC. Indeed, the *Xenopus* studies demonstrate that spindle
68 assembly requires that the CPC interacts with both chromatin and microtubules (Tseng et al.,
69 2010; Wheelock et al., 2017).

70 The CPC displays a dynamic localization pattern during cell division that contributes to
71 its known functions. During mitosis, the CPC localizes to the centromeres during metaphase,
72 where it is required for correcting kinetochore-microtubule (KT-MT) attachments, cohesion
73 regulation and checkpoint regulation (Carmena et al., 2012a; Krenn and Musacchio, 2015;
74 Trivedi and Stukenberg, 2020). It then relocates onto the microtubules to form the spindle
75 midzone required at anaphase for cytokinesis (Adams et al., 2001; Carmena et al., 2012b;
76 Cesario et al., 2006; Chang et al., 2006). In *Drosophila* prometaphase I oocytes, however, the
77 CPC is most abundant on the central spindle, similar to the anaphase midzone of mitotic cells,
78 and is not usually observed at the centromeres (Jang et al., 2005; Radford et al., 2012). Another
79 critical component of the prometaphase meiotic spindle is Subito, a *Drosophila* Kinesin-6 and
80 orthologue of MKLP2 (Giunta et al., 2002). Subito is required for organizing the meiotic central
81 spindle and homologous chromosome bi-orientation in *Drosophila* oocytes (Jang et al., 2005).
82 Subito and INCENP genetically interact and are mutually dependent for their localization (Das et
83 al., 2018; Das et al., 2016; Radford et al., 2012). Based on these observations, a model for

84 spindle assembly in *Drosophila* oocytes is that the CPC activates multiple spindle organizing
85 proteins, including Subito. Hence, the goal in this study was to determine how the chromosomes
86 are involved in this process.

87 To test the hypothesis that the chromosomes recruit and activate the CPC to spatially
88 restrict oocyte spindle assembly, we developed an RNAi-resistant expression system to generate
89 separation-of-function mutants of the CPC. The most thoroughly studied pathways for
90 localization of the CPC to chromosomes involves two histone kinases, Haspin and Bub1, which
91 phosphorylate H3T3 and H2AT120 (Hindriksen et al., 2017) and recruit Survivin and Borealin,
92 respectively, to the inner centromeres. However, we provide evidence that Haspin and Bub1 are
93 not required for spindle assembly in oocyte meiosis. Instead, an interaction between Borealin and
94 the chromatin recruits the CPC to the oocyte chromosomes to initiate kinetochore and spindle
95 assembly. Furthermore, Heterochromatin Protein 1 (HP1) may interact with the CPC in multiple
96 phases of spindle assembly. HP1 colocalizes with the CPC on the chromosomes and then they
97 both move onto the spindle. Thus, our research has revealed a mechanism for how the meiotic
98 chromosomes recruit the CPC for spindle assembly and how the CPC moves to the microtubules.
99 We also propose that within the central spindle, the CPC and HP1 promote the bi-orientation of
100 homologous chromosomes in oocytes.

101 # Results

102 ## Using RNAi resistant transgenes to study factors that regulate CPC localization

103 The *Drosophila* meiotic spindle is composed of two types of microtubules. The
104 kinetochore microtubules (K-fibers) are defined by those that end at a kinetochore, and the
105 central spindle is defined by microtubules that make antiparallel overlaps in the center of the
106 spindle and contain the Kinesin 6 Subito (Jang et al., 2005). The CPC is required for the
107 initiation of spindle assembly by recruiting kinetochore proteins to the centromeres and
108 recruiting microtubules around the chromosomes (Radford et al., 2015; Radford et al., 2012).
109 While the CPC localizes to the centromeres in mitotic cells prior to anaphase (Adams et al.,
110 2001; Cesario et al., 2006; Giet and Glover, 2001), it localizes predominantly to the central
111 spindle in prometaphase I *Drosophila* oocytes (Figure 1A). Centromere CPC localization has
112 only been observed under certain conditions, including live imaging (Costa and Ohkura, 2019)
113 and colchicine-treated oocytes where microtubules are destabilized (Figure 1A). Thus, the CPC
114 can localize to meiotic chromatin in addition to spindle microtubules in metaphase oocytes.

115 To study the relationship between CPC localization patterns and function, we developed
116 a system to target the CPC to distinct chromosomal or spindle locations. Oocyte-specific RNAi
117 was used to knock down *Incenp* instead of using mutants because the CPC is essential for
118 viability. *Incenp* or *aurB* RNAi oocytes fail to recruit kinetochore proteins, such as SPC105R or
119 NDC80 to the centromeres, or recruit microtubules around the chromosomes (Radford et al.,
120 2015; Radford et al., 2012). We constructed an *Incenp* transgene to be RNAi resistant with silent
121 mismatches in the region targeted by shRNA *GL00279* (Figure 1B, Figure S 1). Expressing the
122 RNAi-resistant transgene ($Incenp^{WT\text{-}R}$) rescued the defects in *Incenp* RNAi oocytes, including
123 spindle and kinetochore assembly, homolog bi-orientation, and fertility, restoring them to wild-
124 type levels (Figure 1C, Table 1). Having successfully established this RNAi-resistant system, the

125 *Incenp*$^{WT\text{-}R}$ backbone was used to construct separation-of-function *Incenp* mutants. These mutants
126 were analyzed in either a wild-type (i.e. *Incenp*$^{WT\text{-}R}$ oocytes) or an RNAi background (i.e.
127 *Incenp*$^{WT\text{-}R}$ *Incenp RNAi* oocytes).

128 Targeting the CPC to centromeres is sufficient, but not required, to promote kinetochore 129 microtubule (K-fiber) assembly

130 Borealin and Survivin (known as Deterin in *Drosophila*) targets the CPC to the
131 centromeres in mitotic cells (Carmena et al., 2012b; Hindriksen et al., 2017). Borealin and
132 Survivin interact with the N-terminal domain of INCENP, which is required for centromere
133 localization of the CPC (Jeyaprakash et al., 2007; Klein et al., 2006). We were successful at
134 generating an effective *Deterin* shRNA for oocyte RNAi and found the same phenotype as
135 *Incenp* or *aurB* RNAi oocytes (Figure 1C and D). This result suggests that Deterin plays an
136 important role in targeting INCENP and Aurora B to the chromosomes in *Drosophila* oocytes.
137 To test the function of the CPC at the centromere, we deleted conserved amino acids 22-30 in
138 INCENP (referred to as *Incenp*$^{\Delta CEN}$, Figure 1B, Figure S 1) that corresponds to the centromere
139 targeting domain described in chicken INCENP and is predicted to be required for the interaction
140 with Borealin and Deterin (Ainsztein et al., 1998; Jeyaprakash et al., 2007). In *Incenp*$^{\Delta CEN}$,
141 *Incenp* RNAi oocytes, the INCENP$^{\Delta CEN}$ protein had weak localization to the chromosomes, did
142 not recruit Deterin, or promote spindle assembly (Figure 1E). However, the *Incenp*$^{\Delta CEN}$, *Incenp*
143 RNAi oocytes had an intermediate level of SPC105R localization compared to wild-type or
144 *Incenp, aurB* RNAi or *Deterin* RNAi oocytes (Figure 1C-F). These results suggest that the N-
145 terminal domain of INCENP recruits Deterin and is required for spindle assembly in *Drosophila*
146 oocytes, although some kinetochore assembly is possible without it.

147 To directly test whether centromeric CPC can promote spindle assembly and regulate
148 homolog bi-orientation in oocytes, we targeted the CPC to the centromeric regions. Based on a

149 strategy used in HeLa cells, INCENP was fused to the kinetochore protein MIS12 (Liu et al.,
150 2009). MIS12 loads onto centromeres during prophase (Schittenhelm et al., 2007; Venkei et al.,
151 2012), is independent of other kinetochore proteins (Feijão et al., 2013; Przewloka et al., 2007)
152 and localizes to foci on the chromosomes in wild-type and *Incenp* RNAi oocytes (Figure S 2A)
153 (Głuszek et al., 2015). To target the CPC to the centromeres, the N-terminal amino acids 1-46 of
154 INCENP (the "BS" domain) were replaced with MIS12 (*mis12:Incenp*) (Figure 2A).
155 Surprisingly, when *mis12:Incenp* was expressed in wild-type oocytes, we did not observe
156 centromere localization (Figure 2B). However, the females were sterile due to the failure to
157 complete the two meiotic divisions and initiate the mitotic divisions (Figure S 2B, Table 1). This
158 phenotype demonstrated that the transgene was expressed and toxic to the embryo. When
159 expressing *mis12:Incenp* in *Incenp* RNAi oocytes, however, the fusion protein localized in and
160 around the centromeres and spindle assembly was limited. Kinetochore assembly similar to wild-
161 type and K-fiber formation was observed, which was defined as oocytes with microtubules
162 emanating from the kinetochores (Figure 2B and C, Figure S 2C). These spindles were usually
163 short and lacked a central spindle. These results suggest that targeting INCENP to the
164 centromere regions could only promote kinetochore assembly and K-fiber formation.
165 In the presence of endogenous INCENP, MIS12:INCENP did not localize to the
166 centromeres. To test the possibility that regions outside the BS domain of INCENP negatively
167 regulate centromere localization, we fused MIS12 directly to the INbox domain of INCENP
168 (amino acids 655-755 of the C-terminal domain), which is sufficient to recruit Aurora B (Figure
169 2A) (Bishop and Schumacher, 2002). Expressing unfused *INbox* in the presence of endogenous
170 INCENP had a dominant negative effect on oocyte spindle assembly, causing a diminished
171 spindle (Figure 2D) and sterility (Table 1). This observation suggests that unlocalized INbox has

172 a dominant-negative effect. Similar to observations in mammalian cells (Gohard et al., 2014),
173 INbox could be acting like a competitive inhibitor of INCENP by generating non-productive
174 binding interactions with Aurora B. When expressing *mis12:INbox* in wild-type oocytes,
175 MIS12:INbox was present at the centromeres (Figure 2D). MIS12:INbox was also observed on
176 the spindle, although the mechanism and consequences of this are not known. Phospho-INCENP,
177 which is a marker of Aurora B activity (Salimian et al., 2011), was observed at the central
178 spindle and in the vicinity of the centromeres (Figure 2E), showing MIS12:INbox can
179 successfully recruit and activate Aurora B. Similar to *mis12:Incenp*, when *mis12:INbox* was
180 expressed in *Incenp* RNAi oocytes, SPC105R was recruited, K-fibers formed, but there was not
181 central spindle (Figure 2C, F and G, Figure S 2C). The centromeres were unable to bi-orient and
182 were often clustered together and oriented towards the same pole of a monopolar spindle. These
183 results demonstrate that centromere-targeted CPC is sufficient to build kinetochores and K-
184 fibers, consistent with findings in *Xenopus* extracts (Bonner et al., 2019), but not the central
185 spindle.

186 Independent targeting of the CPC to both the centromere and central spindle is not 187 sufficient to assemble a wild-type spindle

188 Because centromere-directed Aurora B only promotes K-fiber assembly, it is possible
189 that oocyte spindle assembly depends on microtubule-associated Aurora B. Indeed, our prior
190 studies have suggested the CPC is simultaneously required for kinetochore and central spindle
191 microtubule assembly in oocytes (Radford et al., 2015). Therefore, we performed experiments to
192 determine whether the recruitment of Aurora B to these two sites is independent or whether one
193 site might depend on the other. To target Aurora B to the spindle, the *INbox* was fused with two
194 microtubule-associated proteins, Fascetto (*feo*, the *Drosophila* PRC1 homolog) and Subito
195 (Figure 2A). These two fusions, *feo:INbox* and *sub:INbox*, resulted in robust INbox localization

196 to the central spindle when expressed in wild-type oocytes (Figure 2D, E and Figure S 2D).
197 When expressed in *Incenp* RNAi oocytes, neither *feo:INbox* nor *sub:INbox* oocytes assembled a
198 spindle around the chromosomes (Figure 2F and Figure S 2C). These results suggest that
199 microtubule associated Aurora B is not sufficient to promote spindle assembly around the
200 chromosomes. Fusing Subito to the INbox promoted microtubule bundles in the cytoplasm but
201 not in the specifically important location around the chromosomes. Additionally, most SPC105R
202 localization was absent in *sub:INbox, Incenp* RNAi oocytes (Figure 2F, Figure S 2C) similar to
203 *Incenp* RNAi (Figure 1C,F). One possible explanation for these observations is that the central
204 spindle targeting of Aurora B lacked the interaction with the chromosomes necessary for spindle
205 and kinetochore assembly.

206 The problem with the *feo:INbox* and *sub:INbox* experiments could have been the absence
207 of chromosome-associated Aurora B to recruit microtubules and nucleate central spindle
208 assembly. Therefore, to test whether independent targeting of Aurora B to the chromosomes and
209 the microtubules would promote spindle assembly, we co-expressed *mis12:INbox* and either
210 *sub:INbox* or *feo:INbox* in *Incenp* RNAi oocytes. Interestingly, only the K-fibers formed in these
211 oocytes, suggesting that *sub:INbox* and *feo:INbox* cannot contribute to spindle assembly even in
212 the presence of K-fibers (Figure 2G and Figure S 2C). We did observe enhanced microtubule
213 bundling involving the K-fibers, indicating that SUB:INbox was active and could contribute to
214 microtubule bundling. These results indicate that independently targeting two populations of
215 Aurora B is not sufficient to assemble a bipolar spindle (see also Tseng et al., 2010).

216 ## Borealin, but not Deterin, is sufficient for most meiotic spindle assembly

217 Central spindle assembly may require an interaction between the CPC and the
218 chromosomes before the bundling of antiparallel microtubules. Furthermore, the phenotype of
219 *Incenp*$^{\Delta CEN}$ and *Deterin* RNAi oocytes suggests that Borealin and Deterin are critical for

220 chromosome-directed spindle assembly in oocytes (Figure 1D and E). To test whether an
221 interaction of Deterin and/or Borealin with INCENP is sufficient to target the CPC for oocyte
222 spindle assembly, we replaced the BS domain of INCENP with Deterin or Borealin (referred to
223 as *Det:Incenp* and *borr:Incenp*, Figure 3A). In *Det:Incenp* oocytes, INCENP localized to the
224 chromatin close to the centromeres and K-fibers were formed. However, DET:INCENP failed to
225 localize to the spindle and no central spindle was observed (Figure 3B). Borealin localization
226 could not be detected in *Det:Incenp*, *Incenp* RNAi oocytes (Figure S 3A), suggesting this spindle
227 phenotype is independent of Borealin.

228 In contrast, *borr:Incenp* rescued spindle assembly, including the central spindle, in
229 *Incenp* RNAi oocytes (Figure 3B) although the degree of rescue in some oocytes was variable.
230 Some of these oocytes had frayed central spindles (Figure 3C, D) and in 47% oocytes, INCENP
231 localized to the microtubules but failed to be concentrated in the central spindle (n=28, Figure
232 3B). A bipolar spindle also formed when *borr:Incenp* was expressed in *Deterin* RNAi oocytes
233 although similar to *borr:Incenp*, *Incenp* RNAi oocytes, there were some spindle abnormalities
234 (17% diffuse INCENP localization, 48% frayed spindles, Figure 3C and 3D). In contrast, 44% of
235 *Deterin* RNAi oocytes did not assemble a spindle, and the rest only showed non-specific
236 microtubule clustering around the chromosomes (Figure 3C and 3D). Thus, the *borr:Incenp*
237 fusion promotes spindle assembly independent of Deterin. Deterin localized to the spindle in
238 *borr:Incenp*, *Incenp* RNAi oocytes, but only when BORR:INCENP was concentrated in the
239 central spindle (Figure 3E). These observations suggest that Borealin is sufficient to move the
240 CPC from the chromosomes to the microtubules and promote spindle assembly in *Drosophila*
241 oocytes. An important role for Borealin in CPC-dependent spindle assembly has also been shown
242 in *Xenopus* (Kelly et al., 2007). Deterin, in contrast, can promote INCENP localization to the

243 chromatin and K-fiber formation, and may have a role stabilizing the interaction of Borealin and
244 INCENP with microtubules. Deterin is not, however, sufficient to promote movement of the
245 CPC to the microtubules.

246 Recruitment of the CPC to the chromosomes and spindle assembly depends on the C-
247 terminal domain of Borealin

248 Deterin and Borealin are known to be recruited by the histone markers H3T3ph and
249 H2AT120ph, respectively (Wang et al., 2010; Yamagishi et al., 2010). These two histones are
250 phosphorylated by Haspin and BUB1 kinases, respectively. However, spindle assembly and CPC
251 localization were normal in *haspin,* or *Bub1* RNAi oocytes or *haspin, Bub1* double RNAi
252 oocytes, suggesting Haspin and BUB1 are not required for spindle assembly (Figure S 4A). In
253 addition, fertility and chromosome segregation was not affected in any of the genotypes (Figure
254 S 4B), ubiquitous expression of *haspin,* or *Bub1* shRNAs did not cause lethality, and *haspin* null
255 mutants are viable and fertile (Fresan et al., 2020). These results suggest that Haspin and BUB1
256 are not required for the CPC to promote oocyte spindle assembly. Therefore, we investigated
257 other mechanisms for Borealin-mediated CPC recruitment to the chromosomes.

258 In addition to recruitment by BUB1 activity, Borealin can be recruited to chromosomes
259 by an interaction between its C-terminal domain and HP1 (Liu et al., 2014) or nucleosomes
260 (Abad et al., 2019). Although the C-terminal domain of Borealin is poorly conserved, there is
261 evidence in support of the hypothesis that the CPC interacts with HP1 during chromosome-
262 directed spindle assembly in oocytes. INCENP and Borealin colocalize with HP1 and H3K9me3,
263 the histone marker that recruits HP1, in *aurB* RNAi oocytes (Figure 4A and 4B). Furthermore,
264 HP1 is present on chromosomes in *Incenp* RNAi oocytes (Figure 4A), showing that the CPC is
265 not required for HP1 localization. To test the hypothesis that HP1 recruits the CPC to chromatin
266 in oocytes, we deleted the C-terminal domain of Borealin from *borr:Incenp* (referred as

267 *borr$^{\Delta C}$:Incenp*) (Figure 4C). Spindle assembly was severely impaired in *borr$^{\Delta C}$:Incenp*, *Incenp*
268 RNAi oocytes. Only 19% of oocytes assembled K-fibers, and none of them assembled the central
269 spindle (Figure 4D, 4E and 4F). Most of the oocytes that assembled K-fibers (75%) had normal
270 SPC105R localization (Figure 4F, Figure S 3), suggesting that K-fiber formation was associated
271 with SPC105R localization. Because CPC components and HP1 colocalize when Aurora B
272 activity is absent, we favor the interpretation that an interaction between Borealin and HP1 is
273 required to build both K-fibers and the central spindle in oocytes. However, we cannot rule out a
274 role for an interaction between Borealin and the nucleosomes in recruiting the CPC to the
275 chromosomes.

276 Two putative HP1 interaction sites exist in INCENP (Ainsztein et al., 1998; van der Horst
277 and Lens, 2014) and these were deleted to make *Incenp$^{\Delta HP1}$*. While spindle assembly in
278 *borr$^{\Delta C}$:Incenp, Incenp* RNAi was severely affected, spindle assembly in *Incenp$^{\Delta HP1}$*, *Incenp*
279 RNAi oocytes was similar to wild type, except that 36% oocytes INCENP displayed irregular
280 and disorganized central spindle localization (Figure 4D, E, and G). Thus, an INCENP-HP1
281 interaction may only have a minor role in oocyte spindle assembly. To test for additive effects, a
282 mutant with all HP1 sites deleted was generated (*borr$^{\Delta C}$:Incenp$^{\Delta HP1}$*). A more severe spindle
283 assembly defect was observed in *borr$^{\Delta C}$:Incenp$^{\Delta HP1}$*, *Incenp* RNAi oocytes. Specifically, the
284 spindle was abolished in nearly all the oocytes and we measured a small decrease in K-fiber
285 formation ($p = 0.08$, Figure 4D and E). These results suggest that the C-terminal domain of
286 Borealin recruits the CPC to the oocyte chromosomes, with a minor contribution from INCENP.
287 To test whether the only function of Borealin in oocytes is to interact with HP1 for recruitment
288 of the CPC, the BS domain of *Incenp* was replaced with HP1 (*HP1:Incenp*) (Figure 4C).
289 HP1:INCENP localized to part of the chromatin, probably the heterochromatin regions, but 53%

290 of the oocytes failed at spindle assembly, and the rest only had K-fiber formation associated with
291 SPC105R localization (Figure 4E, F and H, Figure S 3). Thus, targeting the CPC to the
292 heterochromatin regions without Borealin is not sufficient for bipolar spindle assembly. Rather
293 than Borealin being an adapter for CPC localization, an interaction between Borealin and HP1
294 and/or nucleosomes appears to be essential for transfer of the CPC to the microtubules and
295 oocyte spindle assembly.

296 Ejection of HP1 and the CPC from the chromosomes depends on Aurora B and 297 microtubules

298 To determine if Borealin is sufficient to target the CPC to the chromatin, we examined
299 the behavior of BORR:INCENP fusion proteins when Aurora B activity was inhibited. Similar to
300 the results in *aurB* RNAi oocytes, when wild-type oocytes were treated with the Aurora B
301 inhibitor Binucleine 2 (BN2) (Smurnyy et al., 2010), the spindle was drastically diminished and
302 INCENP colocalized with HP1 and H3K9me3 on the chromosomes (Figure 5A). The same result
303 was observed with *borr:Incenp*, *Incenp* RNAi oocytes. The BORR:INCENP fusion colocalized
304 with HP1 on the chromosomes in BN2 treated oocytes (Figure 5A). In contrast, in *borr$^{\Delta C}$:Incenp,*
305 *Incenp* RNAi oocytes, the BORR$^{\Delta C}$:INCENP fusion did not localize to the chromosomes. These
306 results suggest the Borealin C-terminal domain is required to target the CPC to the
307 chromosomes, including sites enriched with HP1.

308 In wild-type oocytes, HP1 is on the spindle but in the absence of Aurora B activity is on
309 the chromosomes (Figure 5A). To test if Aurora B activity promotes the transfer of HP1 from the
310 chromosomes to the spindle, we used colchicine to depolymerize the microtubules without
311 inhibiting Aurora B activity. Colchicine treatment caused the CPC to retreat to the chromosomes
312 and colocalize with H3K9me3 in wild-type oocytes (Figure 5B). Chromosome associated
313 INCENP was also observed in colchicine-treated *borr:Incenp*, *Incenp* RNAi, consistent with the

314 conclusion that Borealin promotes CPC localization to the chromosomes. However, HP1 was
315 barely detectable in colchicine-treated wild-type oocytes (Figure 5B), unlike the observation in
316 BN2-treated and *aurB* RNAi oocytes (Figure 5A and Figure 4A and B). These results suggested
317 that Aurora B activity negatively regulates HP1 localization. To test this hypothesis, we
318 compared colchicine treated *Incenp*$^{\Delta HP1}$, *Incenp* RNAi and *borr*$^{\Delta C}$*:Incenp*$^{\Delta HP1}$, *Incenp* RNAi
319 oocytes. In the latter, which fail to recruit Aurora B to the chromosomes, HP1 localized to the
320 chromatin. Because *Incenp*$^{\Delta HP1}$, *Incenp* RNAi oocytes recruit Aurora B to the chromosomes and
321 assemble a spindle with associated HP1 while *borr*$^{\Delta C}$*:Incenp*$^{\Delta HP1}$, *Incenp* RNAi oocytes do not,
322 the most likely explanation is that once HP1 is ejected from the chromosomes, Aurora B activity
323 prevents its return. Thus, the ejection of HP1 from the chromosomes depends on Aurora B
324 activity and Borealin. Ejection of the CPC from the chromosomes, however, depends on Aurora
325 B activity, Borealin, and the microtubules.

326 Recruitment of the CPC to the chromosomes and spindle assembly does not depend on 327 INCENP microtubule interacting domains or Subito

328 We have thus far provided evidence that Borealin targets the CPC to the chromosomes,
329 and then Aurora B activity results in spindle assembly and movement of the CPC to the
330 microtubules. Because CPC localization to the chromosomes depends on the presence of
331 microtubules, we examined if the microtubule binding domains within the CPC promoted
332 spindle localization. INCENP has a single-α-helix (SAH) domain that binds microtubules
333 (Samejima et al., 2015) and a conserved domain within the N-terminal region (the spindle
334 transfer domain, STD) that is required for transfer to the midbody (Ainsztein et al., 1998),
335 possibly by interacting with a kinesin 6 such as MKLP2/ Subito (Serena et al., 2020) (Figure S
336 1). To test if either of these microtubule interaction domains are important for the CPC to
337 relocate and assemble the meiotic spindle, we generated deletions in each site (Figure 6A). In

338 both *Incenp*$^{\Delta STD}$, *Incenp* RNAi and *Incenp*$^{\Delta SAH}$, *Incenp* RNAi oocytes, we observed bipolar
339 spindle assembly and normal CPC localization and a central spindle, suggesting these
340 microtubule binding domains are not required for oocyte meiotic spindle assembly (Figure 6B).
341 However, these females displayed either reduced fertility or sterility (Table 1), suggesting that
342 these two domains of INCENP have an important role in embryonic mitosis. Whether these two
343 domains are redundant in meiosis, or spindle localization of the CPC depends only on Borealin,
344 or another pathway, to interact with microtubules, remains to be investigated.

345 In *Drosophila*, kinesin-6 Subito is required to organize the central spindle, which
346 includes recruiting the CPC (Das et al., 2018; Jang et al., 2005; Radford et al., 2012). However,
347 the CPC can localize to the spindle microtubules in the absence of Subito (Das et al., 2018; Jang
348 et al., 2005) (Figure 6C), suggesting that ejection of the CPC from the chromosomes may be
349 sufficient for spindle transfer and Subito is not required. Interestingly, we found that Subito has a
350 conserved HP1-binding site (amino acid 88-92, PQVFL). To test if the putative Subito HP1
351 binding site is required to build the central spindle, we examined *sub*^{HM26}, a *sub* allele that has a
352 point mutation (L92Q) in the HP1 binding site (Jang et al., 2005). Subito^{HM26} failed to localize to
353 the spindle in oocytes, the spindle displayed a tripolar phenotype and the CPC localized
354 throughout the spindle, all similar to a *sub* null mutant (Figure 6C). Thus, an HP1 interaction
355 may be required for Subito localization, although we have not yet shown a direct interaction
356 between HP1 and Subito.

357 Homolog bi-orientation is regulated through the central spindle and proper spindle 358 localization of the CPC and HP1

359 In mitotic cells, the CPC has an important role in error correction by destabilizing
360 incorrect KT-MT attachments at the centromeres (Carmena et al., 2012b; Funabiki, 2019). Two
361 hypomorphic CPC mutants, *Incenp*^{QA26} and *aurB*^{1689}, could be defective in error correction

362 because they are competent to build a bipolar spindle but have bi-orientation defects in oocytes
363 (Radford et al., 2012; Resnick et al., 2009). Because the CPC in oocytes is most prominent on
364 the central spindle, Aurora B activity could regulate bi-orientation while located on the
365 microtubules rather than the chromosomes. To compare the role of CPC at the centromeres and
366 central spindle in regulating homolog bi-orientation, we used fluorescence in situ hybridization
367 (FISH) to examine three sets of *Incenp* mutants where the CPC is inappropriately localized to
368 either the centromeres or the central spindle. The FISH probes targeted the pericentromeric
369 regions each of chromosomes X, 2 and 3.

370 We first examined a sterile hypomorphic *Incenp* allele, $Incenp^{18.197}$, which was
371 discovered based on genetic interactions with *subito* (Das et al., 2016). In $Incenp^{18.197}$ oocytes,
372 the spindle was moderately diminished and a portion of INCENP was retained on the
373 chromosomes in 67% of the oocytes (n=15) (Figure 7A), suggesting this mutant has a defect in
374 CPC spindle transfer rather than chromosome localization. Using FISH, we determined that
375 $Incenp^{18.197}$ mutant oocytes have homolog bi-orientation defects (11%, n = 42). Second, *Incenp*
376 transgenes with a MYC tag fused to the N-terminus have dominant defects in meiosis (Radford
377 et al., 2012). To investigate whether the N-terminal tag was the cause of this defect, a new set of
378 transgenes were constructed using the RNAi resistant backbone and different tags (MYC, HA
379 and FLAG). We found that regardless of the fused tag, all the transgenes had similar phenotypes:
380 reduced fertility and elevated meiotic nondisjunction in *Incenp* RNAi oocytes (Table 1), and
381 failure to concentrate the CPC to the central spindle (Figure 7A). When the epitope tag was
382 removed to generate $Incenp^{WT\text{-}R}$ (this transgene was the backbone used to generate the mutants in
383 this study), the defects in *Incenp* RNAi oocytes were fully restored to wild-type levels. These

384 results confirmed that the N-terminal epitope tags in INCENP interfered with the CPC's central
385 spindle localization and function.

386 Third, to test which population of the CPC regulates homolog bi-orientation, we used
387 INbox fusions to target overexpression of Aurora B to specific sites. We predicted that
388 overexpression of Aurora B would disrupt bi-orientation by destabilizing KT-MT attachments.
389 Although forcing Aurora B localization to the centromere has been shown to cause bi-orientation
390 defects in mitotic cells (Liu et al., 2009), the frequency of bi-orientation in oocytes expressing
391 *mis12:INbox* was not significantly elevated compared to wild-type (Figure 7B and C). We also
392 tested whether centromere-targeting Aurora B can destabilize microtubules by treating the
393 oocytes with colchicine. K-fibers are more resistant to colchicine treatment than the central
394 spindle, and the amount of K-fibers after colchicine treatment is a measure of attachment
395 stability. The results of colchicine treated wild-type and *mis12:INbox* oocytes were comparable,
396 the spindle was diminished to the same extent, indicating that the stability of the KT-MTs was
397 similar in each genotype (Figure 7D and E). Thus, overexpression of Aurora B activity at the
398 centromeres did not cause bi-orientation defects. In contrast, central-spindle-targeted Aurora B
399 (*sub:INbox* or *feo:INbox*) caused significantly more bi-orientation defects than in wild type
400 (Figure 7B and C). These results suggest that the CPC regulates homolog bi-orientation from
401 within the central spindle rather than at the kinetochores.

402 If targeting the CPC to the central spindle is required for bi-orientation, *Incenp* mutants
403 with defects interacting with microtubules should have bi-orientation defects. Indeed, $Incenp^{\Delta STD}$,
404 *Incenp* RNAi oocytes had homolog bi-orientation defects (Figure 7C), despite having apparently
405 wild-type spindle assembly and CPC localization (Figure 5D). $Incenp^{\Delta HP1}$, *Incenp* RNAi oocytes
406 had wild-type spindle morphology, but had defects in fertility and CPC localization to the central

407 spindle (Figure 4D and G). Interestingly, we found HP1 spindle localization in *Incenp*$^{\Delta HP1}$,
408 *Incenp* RNAi oocytes was different from wild type: HP1 was not enriched in the overlap with the
409 CPC (Figure 7F). Like several of the *Incenp* mutants, *Incenp*$^{\Delta HP1}$ causes a dominant sterile
410 phenotype (Table 1). Therefore, we examined *Incenp*$^{\Delta HP1}$ expressing oocytes by FISH and found
411 these also had a homolog bi-orientation defect (Figure 7B and C). These results are consistent
412 with the model that spindle localization of the CPC and interaction with HP1 is important for
413 regulating homolog bi-orientation.
414 To test HP1 directly, we examined oocytes depleted of HP1 by expressing shRNA
415 *GL00531* because null mutations in HP1 (*Su(var)205* in *Drosophila*), cause lethality. These
416 oocytes displayed wild-type spindles with normal CPC localization (Figure S 4), which could be
417 explained by the relatively mild knockdown of *HP1* (48% of mRNA remains). However,
418 expression of *GL00531* in oocytes caused elevated X-chromosome non-disjunction (8.7%; n =
419 321). These results support the conclusion that during prometaphase I, HP1 and the CPC relocate
420 from the chromosomes to the central spindle where they are both critical for homolog bi-
421 orientation.
422

423 # Discussion

424 *Drosophila* oocytes generate spindles despite lacking centrioles or predefined spindle
425 poles, like in many other organisms. Whether the microtubules assemble around MTOCs as in
426 the mouse (Schuh and Ellenberg, 2007) or more closely around the chromosomes in *Drosophila*
427 and humans (Hadders et al., 2020; Hengeveld et al., 2017), the chromatin appears to play a role
428 in focusing microtubule assembly in the vicinity of, if not contacting, the chromosomes. The
429 chromosome-associated molecules that drive this process, however, are not well known. Our
430 previous studies have shown that the CPC is required for spindle assembly in *Drosophila* oocytes
431 (Radford et al., 2012). We found that the known pathways for recruiting Survivin and Borealin to
432 the centromere via Haspin and Bub1 are not essential for spindle assembly in *Drosophila*
433 oocytes, although we have not ruled out minor roles in spindle assembly. Instead, we found that
434 Borealin targets the CPC to chromatin, consistent with studies in *Xenopus* extracts (Kelly et al.,
435 2007).

436 ## CPC-dependent, chromosome-directed spindle assembly in oocytes depends on a
437 Borealin-chromatin interaction, possibly involving HP1.

438 Although INCENP can recruit HP1 (Kang et al., 2011), several lines of evidence suggest
439 that HP1 can recruit the CPC prior to spindle assembly. When Aurora B is absent or inhibited in
440 *Drosophila* oocytes, a complex of INCENP, Borealin and Survivin colocalizes with HP1 on
441 chromosomes (Figure 5A). HP1 has also been shown to physically interact with the CPC in
442 *Drosophila* (Alekseyenko et al., 2014). In HeLa cells, HP1 promotes CPC localization to
443 chromatin and precedes H3T3 phosphorylation by Haspin kinase (Ruppert et al., 2018). Also in
444 human cells, an interaction between Borealin and nucleosomes (Abad et al., 2019) or HP1 (Liu et
445 al., 2014) recruits the CPC to the chromosomes. Borealin is also sufficient to recruit the CPC to
446 chromatin in *Xenopus* (Kelly et al., 2007). Thus, the evidence from *Drosophila* oocytes and

447 vertebrate cells is consistent and suggests that Borealin interacts with histones and HP1 to recruit
448 the CPC to the chromatin. Possibly aided by HP1 interacting proteins like POGZ (Nozawa et al.,
449 2010), phosphorylation of HP1 (Williams et al., 2019) or H3S10 (Duan et al., 2008; Fischle et
450 al., 2005; Hirota et al., 2005) by Aurora B can promote HP1 ejection from the chromosomes.
451 Thus, Aurora B activity could promote the transfer of a CPC-HP1 complex from the oocyte
452 chromosomes to the microtubules.

453 We propose a model that not only explains how the chromosomes recruit spindle
454 assembly factors, but also how the CPC moves from the chromosomes to the spindle (Figure 8).
455 After nuclear envelope breakdown, a tripartite complex of the CPC comprised of INCENP,
456 Borealin and Survivin/Deterin (Jeyaprakash et al., 2007) is recruited to the chromatin and
457 enriched in regions marked by H3K9me3 and HP1. This localization is independent of Aurora B
458 activity, suggesting that Borealin, in association with INCENP, is responsible for the recruitment
459 of the CPC to HP1 and chromatin. Once the CPC localizes to the chromosomes, Aurora B
460 activity results in phosphorylation of several targets and assembly of the kinetochore. HP1 is
461 then ejected from the chromatin (Figure 4, Figure 5), which could be a mechanism for how the
462 CPC is released from the chromatin and relocates onto the microtubules.

463 This model explains how spindle assembly is restricted to the chromosomes in an
464 acentrosomal system (Ohkura, 2015; Reschen et al., 2012; Rome and Ohkura, 2018); it is based
465 on a Chromatin/HP1-Borealin interaction. We and others have suggested that restricting spindle
466 assembly proximal to the chromosomes involves inhibition of spindle assembly factors in the
467 cytoplasm (Beaven et al., 2017; Das et al., 2018; Rome and Ohkura, 2018). Spindle assembly
468 could involve activating spindle promoting factors such as kinetochore proteins (Emanuele et al.,
469 2008; Haase et al., 2017) and kinesins that bundle microtubules (Beaven et al., 2017; Das et al.,

470 2018). For example, the kinesin NCD that has been shown to be inhibited by 14-3-3, which is
471 released by Aurora B phosphorylation (Beaven et al., 2017). Spindle assembly may also involve
472 suppressing microtubule depolymerases, such as kinesin 13/MCAK and Op18/Stathmin (Kelly et
473 al., 2007; Sampath et al., 2004). We propose that the release of the CPC from the chromosomes
474 locally activates spindle assembly factors.

475 Non-kinetochore microtubules require spindle-associated CPC

476 In mutants where the CPC was targeted to the chromosomes (*mis12:Incenp, Det:Incenp)*,
477 kinetochore assembly and K-fiber formation were observed (Figure 2, Figure 3). In other
478 mutants (*HP1:Incenp* and *Incenp*$^{\Delta CEN}$), only limited kinetochore assembly and K-fibers were
479 observed. Thus, low levels of CPC are sufficient for kinetochore assembly, but higher levels
480 and/or specific localization are required for spindle assembly. Similar conclusions regarding
481 localization and dosage have been made in *Xenopus;* kinetochore assembly can occur without
482 localization of the CPC to the centromeres, may require less Aurora B activity than spindle
483 assembly, and centromeric CPC localization is required for error correction but not for
484 kinetochore assembly (Haase et al., 2017; Kelly et al., 2007; Tseng et al., 2010; Xu et al., 2009).
485 A notable difference compared to *Xenopus,* however, is that the SAH domain is not required for
486 kinetochore assembly in *Drosophila* oocytes (Bonner et al., 2019; Wheelock et al., 2017).

487 The absence of non-kinetochore microtubules in the mutants where the CPC was targeted
488 to the chromosomes suggests spindle assembly requires microtubule associated CPC. For
489 example, the DET:INCENP fusion promotes kinetochore and K-fiber assembly, but no central
490 spindle (Figure 3). Central spindle assembly depends on transfer of the CPC from the
491 chromosomes to the microtubules (Figure 5), and Deterin does not have this activity. The CPC
492 contains multiple spindle-interacting domains, including two in INCENP (STD and SAH) (van
493 der Horst et al., 2015). In addition, it has been proposed that an HP1-INCENP interaction in

494 HeLa cells promotes the transfer of the CPC from the heterochromatin to the spindle (Ainsztein
495 et al., 1998). However, it is possible that Borealin provides this activity in *Drosophila* oocytes.
496 Borealin has a microtubule binding site (Trivedi et al., 2019b), which could drive spindle
497 transfer, and explain how the BORR:INCENP fusion is sufficient for oocyte spindle assembly
498 but the DET:INCENP fusion is not. Deterin has a role in stabilizing the central spindle (Figure 3,
499 Figure 8)

500 Subito is required to promote release of CPC from chromatin in *Drosophila* (Cesario et
501 al., 2006) and human (Serena et al., 2020) mitotic cells, but this is not the case in oocytes. In *sub*
502 mutants, the central spindle is absent but robust bundles of CPC-containing non-kinetochore
503 microtubules form (Jang et al., 2005). These observations suggest the CPC promotes assembly
504 and bundling of microtubules, independent of Subito. When the CPC is ejected from the
505 chromosomes, it may activate the Augmin pathway that has been shown to increase the amount
506 of spindle microtubules in *Drosophila* oocytes (Rome and Ohkura, 2018). Subito, like its human
507 homolog (Adriaans et al., 2020), is required to transport or recruit the CPC to the central spindle.
508 Preventing Subito from interacting with the CPC could be an important regulatory modification
509 in oocytes to ensure that microtubules do not assemble in the absence of chromosomes (Figure
510 6).

511 ## Regulation of Homolog Bi-orientation by the CPC

512 Several previous studies have suggested that chromosome localized CPC regulates error
513 correction, bi-orientation, and checkpoint silencing (Andrews et al., 2004; Foley and Kapoor,
514 2013; Liu et al., 2009; Tanaka et al., 2002), although some of these functions may not require
515 precise centromere localization (Hadders et al., 2020; Hengeveld et al., 2017). However, our
516 analysis of multiple *Incenp* mutants suggests that chromosomal localization of the CPC may not
517 promote these functions. For example, the centromere-targeting of the CPC in meiosis did not

518 cause KT-MT destabilization or affect homolog bi-orientation (Figure 7), as might be predicted
519 if centromere-bound CPC can promote destabilization of microtubule attachments. Instead,
520 several lines of evidence show that mutants with defects specific to spindle localization had the
521 most severe bi-orientation defects (Figure 7). First, we have previously shown that defects in
522 central spindle associated proteins, including actin-associated factors, results in bi-orientation
523 defects (Das et al., 2016). Second, forcing localization of CPC to the central spindle, but not the
524 kinetochores, disrupts bi-orientation. Third, an N-terminal epitope-tag on INCENP caused the
525 CPC to spread out along the spindle, causing defects in homolog bi-orientation and fertility
526 (Radford et al., 2012). These effects are enhanced by a reduction in Subito activity (Das et al.,
527 2016; Radford et al., 2012), consistent with a function for the CPC in the central spindle. Finally,
528 INCENP$^{\Delta STD}$ oocytes had defective homolog bi-orientation, suggesting the conserved spindle
529 transfer domain in INCENP is required for homolog bi-orientation. All these results suggest that
530 defects in the central spindle caused a homolog bi-orientation defect, and are consistent with the
531 hypothesis that homolog bi-orientation of meiotic chromosomes depends on interactions between
532 the CPC and microtubules of the central spindle.

533 An INCENP-HP1 interaction also appear to be important for bi-orientation once the CPC
534 and HP1 moves onto the spindle. Indeed, deleting the HP1 interaction site (121-232 amino acid)
535 of INCENP caused disorganized CPC central spindle localization, loss of HP1 enrichment with
536 the CPC and bi-orientation defects (Figure 4, Figure 7). HP1 or heterochromatin has also been
537 shown to promote accurate achiasmate chromosome segregation during meiosis I in *Drosophila*
538 oocytes (Giauque and Bickel, 2016; Karpen et al., 1996). HP1 interacts with a variety of proteins
539 through its chromo-shadow domain (Eissenberg and Elgin, 2014). Therefore, HP1 could be
540 involved in a complex pattern of interactions that bring important spindle proteins together, such

541 as the CPC and Aurora B phosphorylation substrates such as Subito, which also has a conserved
542 HP1 binding site that is required for its meiotic functions (Figure 7) (Jang et al., 2007; Jang et al.,
543 2005). How this milieu of proteins promotes bi-orientation is still a mystery. The central spindle
544 is a complex structure, containing several proteins that have a microtubule binding domains,
545 including Borealin and INCENP, that may allow the CPC to simultaneously interact with
546 microtubules and regulate KT-MT attachments (Trivedi et al., 2019b; Wheelock et al., 2017).
547 Several *Drosophila* central spindle components have been suggested to form structures by phase
548 separation (So et al., 2019), including HP1 (Liu et al., 2020) and the CPC (Trivedi et al., 2019a).
549 We suggest the central spindle forms a unique structure that allows for the sensing bi-orientation
550 of bivalents.

551 During meiosis I, the pairs of centromeres within a bivalent bi-orient at a much greater
552 distance than the sister centromeres in mitosis or meiosis II. Therefore, it is plausible that the bi-
553 orientation mechanism that works for sister centromeres does not work for homologous
554 centromeres that are significantly further apart and lacking a direct connection. The meiotic
555 central spindle may provide a direct connection between homologous centromeres by combining
556 two properties. The first is a mechanism to coordinate the movement and separate the
557 kinetochores of bivalents. This may be analogous to the activity of "bridging fibers" which can
558 separate pairs of sister kinetochores in mitosis (Simunic and Tolic, 2016; Vukusic et al., 2017).
559 In *C. elegans* meiosis, the central spindle separates homologs for chromosome segregation by
560 microtubule pushing (Laband et al., 2017). The second is a mechanism for microtubule bound
561 CPC to regulate KT-MT attachments and error-correction, which has been observed in several
562 contexts (Fink et al., 2017; Funabiki, 2019; Pamula et al., 2019; Trivedi et al., 2019b). This

563 combination of activities would facilitate allow the central spindle to facilitate reductional

564 chromosome segregation at anaphase I.

Methods and materials

Generation of RNAi resistant INCENP

To engineer RNAi resistant transgenes, we obtained *Incenp* cDNA (RE52507) from *Drosophila* Genomic Resource Center and cloned it into the pENTR vector (Invitrogen, Carlsbad, CA). We used the Change-it Site-directed Mutagenesis kit (Affymetrix) to introduce 8 silent mutations in the region corresponding to amino acids 437-441, which is complementary to *Incenp* shRNA (GL00279). (Figure 1B and Figure S 1). The primers for the site-directed mutagenesis are: 5'-ATGAGCTTTTCAACCCACTCCTGCAGTCGCCCGTCAAGATGCGCGTGGAGGCGTTCGA -3' and 5'-TCGAACGCCTCCACGCGCATCTTGACGGGCGACTGCAGGAGTGGGTTGAAAAGCTCATG -3'. RNAi resistant INCENP constructs including *Incenp*^{myc}, *Incenp*^{HA} and *Incenp*^{Flag} were inserted into the pPMW, pPHW or pPFW vectors that carry the UASp-promoter using the LR Clonase reaction (Gateway, Invitrogen). The construct was then injected in *w* embryos by Model System Injections (Durham, NC). Multiple transgenic lines were selected to balance in a *y w* background and crossed to *mata4-GAL-VP16* with/without *Incenp* RNAi for further testing. The transgenic lines on the 3rd chromosome were chosen for generating a recombinant line with *Incenp* RNAi if the phenotype were comparable with the ones on the X or 2nd chromosome. Expressing *Incenp*^{myc} in an *Incenp* RNAi background rescued spindle assembly and kinetochore assembly in oocytes as well as spindle localization. However, several defects were also observed, such as reduced fertility and elevated X-chromosome nondisjunction and the transgene protein was mislocalized along the spindle instead of concentrating in the central spindle. The same defects were observed previously with an *Incenp*^{myc} variant without the silent mutations (Radford et al., 2012). These results suggest that an epitope tag in the N-terminus of INCENP might

589 interfere with its function, although the HA-tag may have less impact than the other epitopes
590 (Table 1). To solve this problem, a Gibson Assembly kit (New England Biolabs) was used to
591 remove the myc-tag from *Incenp*^{myc} to generate *Incenp*$^{WT\text{-}R}$. Expressing *Incenp*$^{WT\text{-}R}$ in *Incenp*
592 RNAi oocytes displayed wild-type spindle and localization, and restored fertility to wild-type
593 levels. We used a plasmid carrying *Incenp*$^{WT\text{-}R}$ as the backbone for Gibson assembly reactions to
594 generate all the *Incenp* mutations and fusions used in this study. For each mutation, at least two
595 transgenic lines were analyzed for the ability to rescue *Incenp* RNAi with shRNA GL00279.
596 INbox constructs were generated by taking the last 101 amino acids (655-755) of
597 INCENP including INbox and TSS activation site. Fusion proteins of INCENP were created by
598 using MIS12 cDNA (RE19545), Deterin cDNA (LP03704), Su(var)205 cDNA (LD10408) and
599 Borealin cDNA (LD36125). The constructs were injected into *Drosophila y w* embryos by
600 Model System Injections (Durham, NC).

601 ***Drosophila* genetics and generation of shRNA transgenics**

602 Flies were crossed and maintained on the standard media at 25°C. All loci information
603 was obtained from Flybase. Fly stocks were obtained from the Bloomington Stock Center or the
604 Transgenic RNAi Project at Harvard Medical School (TRiP, Boston, USA), including *aurB*
605 (GL00202), *Incenp* (GL00279), *haspin* (GL00176), *Su(var)205* (GL00531) and *Bub1*
606 (GL00151), except *mis12::EGFP* (Głuszek et al., 2015). To generate *Deterin* (LW501) and
607 *haspin* (HK420) shRNA lines, a *Deterin* sequence (5'- CGGGAGAATGAGAAGCGTCTA -3')
608 or a *haspin* sequence (5'- GGAAGACAGTAGAGACAAATG- 3') were cloned into
609 pVALIUM22 following the protocols described by the Harvard TRiP center. The construct was
610 injected into *Drosophila* embryos (*y sc v; attP40*).

611 The pVALIUM22 vector carries the UASp promoter allowing for expression of short
612 hairpins for RNA silencing and transgenes using the UAS/GAL4 binary expression system
613 (Rorth et al., 1998). All the shRNA lines and transgenes used in this paper were expressed by
614 *mata4-GAL-VP16*, which induces expression after early pachytene throughout most stages of
615 oocyte development in *Drosophila* (Sugimura and Lilly, 2006).

616 For quantifying the knockdown of these RNAi lines, total RNA was extracted from late-
617 stage oocytes using TRIzol® Reagent (Life Technologies) and reverse transcribed into cDNA
618 using the High Capacity cDNA Reverse Transcription Kit (Applied Biosystems). The qPCR was
619 performed on a StepOnePlus™ (Life Technologies) real-time PCR system using TaqMan® Gene
620 Expression Assays (Life Technologies). Dm03420510_g1 for *haspin*, Dm02141491_g1 for
621 *Deterin*, Dm01804657_g1 for *Bub1*, Dm0103608_g1 for *Su(var)205* and Dm02134593_g1 for
622 the control *RpII140*. The knockdown of the respective mRNAs in these oocytes was reduced to
623 15% in *haspin* HK420 RNAi oocytes, 32% in *haspin* GL00176 RNAi oocytes, 5% in *Deterin*
624 LW501 RNAi oocytes, 2% in *Bub1* GL00151 RNAi oocytes and 48% in *Su(var)205* GL00531
625 RNAi oocytes. To test for effects on mitosis, shRNA lines were tested for lethality when under
626 the control of *P{tubP-GAL4}LL7,* which results in ubiquitous expression.

627 **Antibodies and immunofluorescence microscopy**

628 To collect images of the meiotic spindle, oocytes were collected from 100-200, 3-4 day
629 old yeast-fed non-virgin females. The protocol for fixation and immunofluorescence of stage 14
630 oocytes has been described (Radford and McKim, 2016). To observe whether spindle assembly
631 was affected in post-meiotic mitosis, embryos were collected from several hundreds of yeast-fed
632 females for 2 hours. After removing chorion by treated embryos with 50% bleach for 90 seconds,
633 embryos then moved to tubes containing 500 µL heptane and 500 µL methanol and shaken

634 vigorously for 30 seconds to fix. Rehydrated embryos were processed for immunofluorescence
635 microscopy. Hoechst 33342 (10 µg/ml, Invitrogen) was used for staining DNA and mouse anti-a
636 tubulin monoclonal antibody DM1A (1:50) conjugated with FITC (Sigma, St. Louis) was used
637 for staining microtubules. Primary antibodies used in this paper were rabbit anti-CID (1:1000,
638 Active motif), rabbit anti-SPC105R (1:4000, (Schittenhelm et al., 2007)), rabbit anti-CENP-C
639 (1:5000, (Heeger et al., 2005)), mouse anti-Myc (1:50, 9E10, Roche, Indianapolis), mouse anti-
640 Flag (1:500, Thermo Fisher), rat anti-INCENP (1:400, (Wu et al., 2008)), rabbit anti-Aurora B
641 (1:1000, (Giet and Glover, 2001)), rabbit anti-Survivin (1:1000, (Szafer-Glusman et al., 2011)),
642 rabbit anti-Borealin (1:100, (Gao et al., 2008)), mouse anti-HP1 (1:50, C1A9, Developmental
643 Hybridoma Bank), rabbit anti-H3K9me3 (1:1000, Active motif), rat anti-Subito (1:75, (Jang et
644 al., 2005)), rat anti-a-tubulin (Clone YOL 1/34, Millipore) and rabbit anti-pINCENP (1:1000,
645 (Salimian et al., 2011)). The secondary antibodies including Cy3 and AlexFluor647 (Jackson
646 Immunoresearch West Grove, PA) or AlexFluor488 (Molecular Probes) were used in accordance
647 with the subjected primary antibodies. FISH probes for the X-chromosome (359 repeats), 2nd
648 chromosome (AACAC satellite) and 3rd chromosome (dodeca satellite) and conjugated to either
649 Alexa Flour 594, Cy3 or Cy5 were obtained from Integrated DNA Technologies (Dernburg et
650 al., 1996; Radford and McKim, 2016). Oocytes were mounted in SlowFade Gold (Invitrogen).
651 Images were collected on a Leica TCS SP8 confocal microscope with a 63x, NA 1.4 lens and
652 shown as maximum projections of complete image stacks. Images were then cropped in Adobe
653 Photoshop.

654 Drug treatment assays

655 To inhibit Aurora B Kinase activity, oocytes were treated by either 0.1% DMSO or 50
656 µM BN2 in 0.1% DMSO in 60 minutes before fixation in Robb's media. To depolymerize

657 microtubules, oocytes were incubated in 250 μM colchicine in 0.5% ethanol or only 0.5%
658 ethanol as a control for either 30 or 60 minutes before fixation depends on whether we wanted to
659 destabilize spindle microtubules (Figure 7) or completely remove all spindle microtubules
660 (Figure 1 and Figure 5).

661 ## X-chromosome nondisjunction assays

662 To determine whether each *Incenp* mutant transgenes affected meiotic chromosome
663 segregation, we measured fertility and X-chromosome nondisjunction. Transgenic virgin females
664 were generated by crossing *mata4-GAL-VP16* to either the *Incenp* transgene or the *Incenp*
665 transgene with *Incenp* RNAi or other RNAi lines. These transgenic females were crossed to *y*
666 *Hw w/B^{S}Y* males. The males carry a dominant mutation, *Bar*, on the Y chromosome which makes
667 chromosome mis-segregation phenotypically distinguishable in the progeny. Crosses were set in
668 vials and fertility was measured based on the progeny number. To compensate for the inviability
669 of nullo-X and triplo-X progeny, the nondisjunction rate was calculated as 2*(XXY and XO
670 progeny)/ total progeny, where total progeny was 2*(XXY and XO progeny)+ XX and XY
671 progeny.

672 ## Image analysis and statistics

673 To measure kinetochore localization, SPC105R foci were identified based on size and
674 intensity and then counted using Imaris image analysis software (Bitplane) with the parameters
675 used in Wang et. al. (Wang et al., 2019). To determine whether HP1 and the CPC were
676 colocalized, line scans were drawn from pole to pole across the central spindle. The intensities of
677 HP1 and Deterin were measured by using Leica SP8 software. In addition, the colocalizing
678 region is shown in Figure 7F. When measuring bi-orientation by FISH, each data point
679 corresponds to one pair of homologous chromosomes. Homologous chromosomes were

680 considered bi-oriented if two FISH signals localized at the opposite ends of chromosome mass.
681 Pairs of homologous chromosomes on the same side of the spindle were considered to have a bi-
682 orientation defect. The appropriate statistical tests for each experiment as indicated in the figure
683 legends were performed using Prism software (GraphPad).

Acknowledgements

We thank Li Nguyen for technical assistance, Christian Lehner, James Wakefield and Michael Lampson for providing antibodies, and Karen Schindler, Ruth Steward for helpful comments and advice. We also thank Sarah Radford for early work on this project and comments on the manuscript. We thank the TRiP at Harvard Medical School for providing transgenic RNAi fly stocks used in this study. Fly stocks obtained from the Bloomington *Drosophila* Stock Center (NIH P40OD018537) were also used in this study. L.W. was funded by a Busch Predoctoral Fellowship. This work was supported by NIH grant GM101955 to K.S.M.

697 Table 1: Summary of transgene fertility

Genotype	Fertility / nondisjunction [1]	
	in wild-type oocytes	**in *Incenp* RNAi oocytes**
Myc:Incenp	+++/ 1.4% NDJ (n=862)	+/ 11.4% NDJ (n=184)
HA:Incenp	+++/ 0.5% (n=552)	+/ 1.3% (n=315)
Flag:Incenp	++/ 5.2% (n=771)	+/ 8.1% (n=150)
Incenp^{WT-R}	+++/ 0% (n=267)	+++/ 0.9% (n=3806)
Incenp$^{\Delta CEN}$	+/ 0% (n=35)	sterile
Incenp$^{\Delta STD}$	Sterile	++/0% (n=323)
Incenp$^{\Delta SAH}$	+/ 0% (n=111)	Sterile
Det:Incenp	Sterile	sterile
Mis12:Incenp	Sterile	sterile
Mis12:Inbox	Sterile	sterile
Feo:Inbox	Sterile	sterile
Sub:Inbox	Sterile	sterile
Inbox	Sterile	sterile
Incenp $^{\Delta HP1}$	Sterile	sterile
HP1:Incenp	++/ 0% (n=113)	sterile
Borr:Incenp	+/ 0% (n=74)	+/ 0% (n=18)
Borr$^{\Delta c}$:Incenp	Sterile	Sterile
Borr $^{\Delta c}$:Incenp $^{\Delta HP1}$	Sterile	Sterile
Wild type	+++/ (n=240)	Sterile

698 [1] Females were crossed to *y Hw w/BSY males* in vials. Fertility is based on the number of
699 progeny per vial: +++ = 20-50 per vial, ++ = 10-20 per vial and + = 1-10 per vial and sterile =
700 no progeny. Nondisjunction = 2XNDJ/total progeny.

701

Figure legends

Figure 1**: INCENP localization and spindle assembly depends on the N-terminal Borealin/Deterin binding domain.**

(A) INCENP localization in oocytes after a 60 minute colchicine treatment to destabilize the microtubules. The sister centromeres appeared to be separating in colchicine treated oocytes, the mechanism of which is not known. INCENP is in red, CID/CENP-A is in white, tubulin is in green and DNA is in blue. Scale bars in all images are 5 µm. (B) A schematic of *Drosophila* INCENP, showing the location of the centromere-targeting N-terminal region (BS), single alpha helix (SAH) and INbox (IN) domains. The black box (437-441) shows the sequence targeted by the shRNA *GL00279* that were mutated to make RNAi resistant $Incenp^{WT\text{-}R}$. The conserved amino acids 22-30 are deleted in $Incenp^{\Delta CEN}$. (C) INCENP (red) localization in *Incenp* RNAi oocytes and oocytes also expressing the $Incenp^{WT\text{-}R}$ RNAi-resistant transgene. Kinetochore protein SPC105R is in white. (D) Spindle and kinetochore assembly defects in *Deterin* RNAi oocytes. (E) Spindle and kinetochore assembly defects in $Incenp^{\Delta CEN}$, *Incenp* RNAi oocytes, with Deterin or INCENP in red and SPC105R or CID in white. (F) Quantitation of SPC105R localization in RNAi oocytes (n=7, 14, 32, 12 22 and 8 oocytes). Error bars indicate 95% confidence intervals and ** = p-value < 0.001 run by Fisher's exact test.

Figure 2**: Independent localization of the CPC to the centromere and the central spindle assembles only kinetochore-dependent microtubules.**

(A) A schematic of the CPC constructs designed to target the CPC to the centromeres. (B) Expression of *mis12:Incenp* in wild-type and *Incenp* RNAi oocytes. (C) Quantitation of the spindle phenotype of MIS12 fusions expressed in *Incenp* RNAi oocytes (n=23, 36 and 25 oocytes). (D) *Myc:INbox*, *Flag:mis12:INbox* and *Myc:sub:INbox* expressed in wild-type oocytes. (E) Detection of the Aurora B substrate, phosphorylated INCENP (pINCENP). The arrow and inset shows the pINCENP signal at the centromeres when the INbox is targeted by MIS12. INCENP is in red and pINCENP is in white. (F) *Flag:mis12:INbox* and *Myc:sub:INbox* expressed in *Incenp* RNAi oocytes. The arrow points to K-fibers in *Flag:mis12:Inbox* oocytes. The low magnification image of *Myc:sub:INbox* shows microtubule bundles in the cytoplasm instead of around the chromosomes. Transgene proteins are in red, SPC105R in white, DNA is in blue and tubulin is in green. Scale bars represent 5 µm in the left three panels and 10 µm in the low magnification image. (G) *Flag:mis12:INbox* expressed alone or co-expressed with *Myc:sub:INbox* in *Incenp* RNAi oocytes. Merged images showed DNA (blue), tubulin (green), Myc (red) and Aurora B (white). Scale bars indicate 5 µm.

738 Figure 3**: Borealin is sufficient to recruit the CPC for meiotic spindles assembling.**

739 (A) A schematic of the *Det:Incenp* and *borr:Incenp* fusions compared to wild-type *Incenp*. (B)
740 The spindle phenotypes of *borr:Incenp* and *Det:Incenp* in *Incenp* RNAi oocytes. The separate
741 channels show the localization of INCENP and the microtubules. The second *borr:Incenp* image
742 is an example of a spindle with diffuse spindle INCENP. Arrows show K-fibers in *Det:Incenp*
743 oocytes and central spindle fibers in *borr:Incenp* oocytes. INCENP is in red, DNA is in blue,
744 tubulin is in green and CID is in white. (C, D) The effect of Deterin depletion in *borr:Incenp*
745 oocytes (n=18 ,23 and 24). (E) Deterin localization in wild-type and *borr:Incenp*, *Incenp* RNAi
746 oocytes. Second *borr:Incenp* image is an example of a spindle with diffuse spindle INCENP.
747 INCENP is in red, Deterin is in white, DNA is in blue and tubulin is in green. Scale bars in all
748 images are 5 µm.

749

750 Figure 4**: HP1-Borealin interaction is critical for CPC-dependent meiotic spindle assembly.**

751 (A) Borealin and HP1 localization in wild type, *Incenp* RNAi and *aurB* RNAi oocytes. Borealin
752 is in white, HP1 is in red, tubulin is in green and DNA is in blue. (B) HP1 and H3K9me3
753 localization in wild-type and *aurB* RNAi oocytes. Arrow shows HP1 localization in wild-type
754 oocytes on the spindle. HP1 or tubulin is in green, INCENP is in red, DNA is in blue and CID or
755 H3K9me3 are in white. (C) A schematic of *Incenp* mutant constructs affecting HP1 interactions.
756 Proposed HP1 binding sites are located in the C-terminus of Borealin and in INCENP between
757 amino acids 121-232. Full length *Drosophila* HP1 was fused to INCENP by substitution for the
758 BS domain. (D) Expression of *Incenp* transgenes shown in (C) in *Incenp* RNAi oocytes,
759 including $borr^{\Delta C}$*:Incenp*, $Incenp^{\Delta HP1}$ and $borr^{\Delta C}$*:*$Incenp^{\Delta HP1}$. Two different images of $Incenp^{\Delta HP1}$
760 are shown to compare ring-shaped and disorganized (see arrow) localization of the CPC. The
761 images show CID in white, INCENP in red, DNA in blue and tubulin in green. (E) Quantitation
762 of spindle phenotype in the HP1-interaction-defective mutants shown in (D) (n= 17, 26, 31 and
763 49 oocytes, in the order as shown in the graph). (F) SPC105R localization (see Figure S 3) in the
764 HP1-interaction-defective mutant oocytes (n= 8, 32, 9, 15, 14, 33). Bars indicates 95%
765 confidence intervals and ** = *p*-value < 0.01 in Fisher's exact test. (G) Quantitation of INCENP
766 spindle localization in wild-type (n=19) and $Incenp^{\Delta HP1}$, *Incenp* RNAi oocytes (n=17). **** = *p*-
767 value < 0.0001. (H) Expressing *HP1:Incenp* (see C) in *Incenp* RNAi oocytes. The images show
768 CID in white, INCENP in red, DNA in blue and tubulin in green.

769

770 Figure 5**: The dissociation of HP1 and the CPC from the chromosomes depends on**
771 **microtubules.**

772 (A) Wild-type oocytes were treated with DMSO (left panel) or BN2 (right panel) for one hour to
773 inhibit Aurora B kinase activity. In red are heterochromatic marks HP1 or H3K9me3 and in
774 white are the CPC components INCENP or Deterin. In all the images, scale bars represent 5 µm.
775 (B) Wild-type oocytes were treated for 60 minutes with ethanol or Colchicine to depolymerize
776 microtubules and analyzed for the same markers as in (A). In all images, DNA is in blue and
777 tubulin is in green.

778

779 Figure 6**: Analysis of CPC interactions with Subito and microtubules required for central**
780 **spindle assembly.**

781 (A) A schematic showing two INCENP deletions removing regions that promote microtubule
782 interactions. (B) Bipolar spindle assembly when *Incenp*$^{\Delta STD}$ or *Incenp*$^{\Delta SAH}$ were expressed in
783 *Incenp* RNAi oocytes. CID is in white, INCENP is in red, Tubulin is in green, DNA is in blue.
784 (C) Tripolar spindle and mislocalization of the CPC phenotype in *sub*^{HM26}/*sub*^{131} oocytes, with
785 tubulin (green), Deterin (white), HP1 or Subito (red) localization. Scale bar is 5 µm in all
786 images.

787

788 Figure 7: **Disruption of homolog bi-orientation by disruptions of central spindle CPC.**

789 (A) Disorganized or mislocalized CPC in the *Incenp* hypomorphic allele *Incenp*$^{18.197}$ and the
790 transgenes *myc:Incenp and HA:Incenp*. The CPC or MYC are in red, CID is in white, tubulin is
791 in green and DNA is in blue. (B) *Incenp* mutants examined for homolog bi-orientation using
792 FISH with probes against pericentromeric heterochromatin on the X (359 bp repeat, yellow), 2nd
793 (AACAC, red) and 3rd (dodeca, white) chromosomes. (C) Rates of bi-orientation defects were
794 quantified (n= 57, 37, 50, 30, 69, 60 and 63 in the order of the graph). * = *p*-value < 0.05 ****=
795 *p*-value <0.0001 in Fisher's exact test. (D) Wild type oocytes and *mis12:INbox* oocytes treated
796 with colchicine for 30 minutes. INCENP is in red and CID is in white. (E) Quantitation of
797 spindle assembly after colchicine treatment (n= 5, 10, 7 and 17 in the order of the graph). (F)
798 Localization of HP1 and Deterin in wild-type and *Incenp*$^{\Delta HP1}$, *Incenp* RNAi oocytes. HP1 is in
799 green, Deterin is in red and overlapping region is in yellow.

800

801 Figure 8: **Model for spindle assembly in *Drosophila* oocytes.**

802 After Nuclear Envelope breakdown, a complex of INCENP, Borealin and Deterin / Survivin is
803 recruited to the chromosomes. Localization studies suggest that CPC recruitment is enriched in
804 heterochromatic regions containing H3K9me3 and HP1. Aurora B is recruited, which results in
805 kinetochore assembly, limited microtubule recruitment in the form of K-fibers, and
806 phosphorylation of other targets including H3S10 and possibly HP1. Aurora B activity also
807 results in Borealin-dependent ejection of HP1 and the CPC from the chromosomes to the
808 microtubules, although the target that is phosphorylated is not known. Once on the microtubules,
809 the Kinesin 6 Subito causes enrichment of the CPC and HP1 in the central spindle.

810

811 Figure S 1**: Alignment and domain analysis of *Drosophila*.**

812 The sequence alignment compares *D. melanogaster* INCENP to *D. virilis* and *X. laevis.* The
813 Borealin/ Deterin binding domain is from amino acids 1-46 (yellow). The *CEN* and *STD* deletion
814 mutations are marked red, two potential HP1 interaction sites are marked in blue, the RNAi
815 mismatch region is marked in black, the SAH domain is marked in orange, and the INbox (IN) is
816 in black.

817

818 Figure S 2**: Expression of *mis12:INbox* in the wild-type oocytes disrupts meiotic**
819 **progression.**

820 (A) MIS12 localization in wild type and *Incenp* RNAi oocytes (arrows). MIS12 is in red, tubulin
821 is in green, DNA is in blue, CENP-C is in white, and the scale bar represents 5 µm. (B) Fertilized
822 0-2hr old *Drosophila* embryos were fixed and stained for INCENP (red), tubulin (green) and
823 DNA (blue). The scale bar is 5 µm. (C) Quantitation of SPC105R localization in oocytes with
824 *mis12* fusions (n= 6, 9,12 oocytes). Error bars indicate 95% confidence intervals and ** = *p*-
825 value < 0.01 run by Fisher's exact test. (D) Expression of *Myc:feo:INbox* in wild-type and
826 *mis12:INbox*, *Incenp*^{RNAi} oocytes. *Myc:feo:INbox* localizes to the central spindle in the wild-
827 type oocytes. (E) Co-expression of *FLAG:mis12:INbox* and *Myc:feo:INbox* in *Incenp* RNAi
828 oocytes. In these images, the Myc tag (FEO:INbox) is red, Aurora B or CID is white, tubulin is
829 green and DNA is blue. The scale bar is 5 µm.

830

831 Figure S 3**: Borealin localization in *Det:Incenp, Incenp* RNAi oocytes and the localization of**
832 **the CPC to the chromosmes.**

833 (A) Metaphase I oocytes from wild-type and *Det:Incenp, Incenp* RNAi females. Borealin is in
834 white, INCENP is in red, tubulin is in green and DNA is in blue. Scale bar is 5 µm. (B)
835 Expression of *Incenp* transgenes shown in (Figure 4C) in *Incenp* RNAi oocytes, including
836 *borr*$^{\Delta C}$*:Incenp*, *Incenp*$^{\Delta HP1}$ and *borr*$^{\Delta C}$*:Incenp*$^{\Delta HP1}$. The images show SPC105R in white,
837 INCENP in red, DNA in blue and tubulin in green. Scale bars represent 5 µm.

838

839 Figure S 4: **Phenotype of *haspin, Bub1* and *Su(var)205* (*HP1*) knockdowns.**

840 (A) Metaphase I oocytes from *haspin or Bub1 single RNAi* or *haspin, Bub1* double RNAi
841 females. Centromere protein CID is in white, INCENP is in red, tubulin is in green and DNA is
842 in blue. Scale bar is 5 µm. (B) Fertility and X-chromosome nondisjunction in *haspin* and *Bub1*
843 RNAi females. G) Spindle in *Drosophila* HP1 mutant, *Su(var)205* (*HP1*) RNAi oocytes. CID is
844 in white, INCENP is in red, tubulin is in green and DNA is in blue. Scale bars in all images are 5
845 µm.

846

847

Literature cited

Abad, M.A., J.G. Ruppert, L. Buzuk, M. Wear, J. Zou, K.M. Webb, D.A. Kelly, P. Voigt, J. Rappsilber, W.C. Earnshaw, and A.A. Jeyaprakash. 2019. Borealin-nucleosome interaction secures chromosome association of the chromosomal passenger complex. *J Cell Biol*. 218:3912-3925.

Adams, R.R., H. Maiato, W.C. Earnshaw, and M. Carmena. 2001. Essential roles of Drosophila inner centromere protein (INCENP) and aurora B in histone H3 phosphorylation, metaphase chromosome alignment, kinetochore disjunction, and chromosome segregation. *J Cell Biol*. 153:865-880.

Adriaans, I.E., P.J. Hooikaas, A. Aher, M.J.M. Vromans, R.M. van Es, I. Grigoriev, A. Akhmanova, and S.M.A. Lens. 2020. MKLP2 Is a Motile Kinesin that Transports the Chromosomal Passenger Complex during Anaphase. *Curr Biol*. 30:2628-2637 e2629.

Ainsztein, A.M., S.E. Kandels-Lewis, A.M. Mackay, and W.C. Earnshaw. 1998. INCENP centromere and spindle targeting: identification of essential conserved motifs and involvement of heterochromatin protein HP1. *J Cell Biol*. 143:1763-1774.

Alekseyenko, A.A., A.A. Gorchakov, B.M. Zee, S.M. Fuchs, P.V. Kharchenko, and M.I. Kuroda. 2014. Heterochromatin-associated interactions of Drosophila HP1a with dADD1, HIPP1, and repetitive RNAs. *Genes Dev*. 28:1445-1460.

Andrews, P.D., Y. Ovechkina, N. Morrice, M. Wagenbach, K. Duncan, L. Wordeman, and J.R. Swedlow. 2004. Aurora B regulates MCAK at the mitotic centromere. *Dev Cell*. 6:253-268.

Beaven, R., R.N. Bastos, C. Spanos, P. Rome, C.F. Cullen, J. Rappsilber, R. Giet, G. Goshima, and H. Ohkura. 2017. 14-3-3 regulation of Ncd reveals a new mechanism for targeting proteins to the spindle in oocytes. *J Cell Biol*. 216:3029-3039.

Bennabi, I., M.E. Terret, and M.H. Verlhac. 2016. Meiotic spindle assembly and chromosome segregation in oocytes. *J Cell Biol*. 215:611-619.

Bishop, J.D., and J.M. Schumacher. 2002. Phosphorylation of the carboxyl terminus of inner centromere protein (INCENP) by the Aurora B Kinase stimulates Aurora B kinase activity. *J Biol Chem*. 277:27577-27580.

Bonner, M.K., J. Haase, J. Swinderman, H. Halas, L.M. Miller Jenkins, and A.E. Kelly. 2019. Enrichment of Aurora B kinase at the inner kinetochore controls outer kinetochore assembly. *J Cell Biol*. 218:3237-3257.

Carmena, M., X. Pinson, M. Platani, Z. Salloum, Z. Xu, A. Clark, F. Macisaac, H. Ogawa, U. Eggert, D.M. Glover, V. Archambault, and W.C. Earnshaw. 2012a. The chromosomal passenger complex activates Polo kinase at centromeres. *PLoS Biol*. 10:e1001250.

Carmena, M., M. Wheelock, H. Funabiki, and W.C. Earnshaw. 2012b. The chromosomal passenger complex (CPC): from easy rider to the godfather of mitosis. *Nat Rev Mol Cell Biol*. 13:789-803.

Cesario, J.M., J.K. Jang, B. Redding, N. Shah, T. Rahman, and K.S. McKim. 2006. Kinesin 6 family member Subito participates in mitotic spindle assembly and interacts with mitotic regulators. *J Cell Sci*. 119:4770-4780.

Chang, C.J., S. Goulding, R.R. Adams, W.C. Earnshaw, and M. Carmena. 2006. Drosophila Incenp is required for cytokinesis and asymmetric cell division during development of the nervous system. *J Cell Sci*. 119:1144-1153.

Cheeseman, I.M. 2014. The kinetochore. *Cold Spring Harbor perspectives in biology*. 6:a015826.

Colombié, N., C.F. Cullen, A.L. Brittle, J.K. Jang, W.C. Earnshaw, M. Carmena, K. McKim, and H. Ohkura. 2008. Dual roles of Incenp crucial to the assembly of the acentrosomal metaphase spindle in female meiosis. *Development*. 135:3239-3246.

894 Costa, M.0F.A., and H. Ohkura. 2019. The molecular architecture of the meiotic spindle is remodeled
895 during metaphase arrest in oocytes. *J Cell Biol*. 218:2854-2864.
896 Das, A., J. Cesario, A.M. Hinman, J.K. Jang, and K.S. McKim. 2018. Kinesin 6 Regulation in Drosophila
897 Female Meiosis by the Non-conserved N- and C- Terminal Domains. *G3 (Bethesda, Md*. 8:1555-
898 1569.
899 Das, A., S.J. Shah, B. Fan, D. Paik, D.J. DiSanto, A.M. Hinman, J.M. Cesario, R.A. Battaglia, N. Demos, and
900 K.S. McKim. 2016. Spindle Assembly and Chromosome Segregation Requires Central Spindle
901 Proteins in Drosophila Oocytes. *Genetics*. 202:61-75.
902 Dernburg, A.F., J.W. Sedat, and R.S. Hawley. 1996. Direct evidence of a role for heterochromatin in
903 meiotic chromosome segregation. *Cell*. 86:135-146.
904 Drutovic, D., X. Duan, R. Li, P. Kalab, and P. Solc. 2020. RanGTP and importin beta regulate meiosis I
905 spindle assembly and function in mouse oocytes. *EMBO J*. 39:e101689.
906 Duan, Q., H. Chen, M. Costa, and W. Dai. 2008. Phosphorylation of H3S10 blocks the access of H3K9 by
907 specific antibodies and histone methyltransferase. Implication in regulating chromatin dynamics
908 and epigenetic inheritance during mitosis. *J Biol Chem*. 283:33585-33590.
909 Dumont, J., and A. Desai. 2012. Acentrosomal spindle assembly and chromosome segregation during
910 oocyte meiosis. *Trends Cell Biol*. 22:241-249.
911 Dumont, J., K. Oegema, and A. Desai. 2010. A kinetochore-independent mechanism drives anaphase
912 chromosome separation during acentrosomal meiosis. *Nat Cell Biol*. 12:894-901.
913 Eissenberg, J.C., and S.C. Elgin. 2014. HP1a: a structural chromosomal protein regulating transcription.
914 *Trends Genet*. 30:103-110.
915 Emanuele, M.J., W. Lan, M. Jwa, S.A. Miller, C.S. Chan, and P.T. Stukenberg. 2008. Aurora B kinase and
916 protein phosphatase 1 have opposing roles in modulating kinetochore assembly. *J Cell Biol*.
917 181:241-254.
918 Feijão, T., O. Afonso, A.F. Maia, and C.E. Sunkel. 2013. Stability of kinetochore-microtubule attachment
919 and the role of different KMN network components in Drosophila. *Cytoskeleton (Hoboken, N.J*.
920 70:661-675.
921 Fink, S., K. Turnbull, A. Desai, and C.S. Campbell. 2017. An engineered minimal chromosomal passenger
922 complex reveals a role for INCENP/Sli15 spindle association in chromosome biorientation. *J Cell*
923 *Biol*. 216:911-923.
924 Fischle, W., B.S. Tseng, H.L. Dormann, B.M. Ueberheide, B.A. Garcia, J. Shabanowitz, D.F. Hunt, H.
925 Funabiki, and C.D. Allis. 2005. Regulation of HP1-chromatin binding by histone H3 methylation
926 and phosphorylation. *Nature*. 438:1116-1122.
927 Foley, E.A., and T.M. Kapoor. 2013. Microtubule attachment and spindle assembly checkpoint signalling
928 at the kinetochore. *Nat Rev Mol Cell Biol*. 14:25-37.
929 Fresan, U., M.A. Rodriguez-Sanchez, O. Reina, V.G. Corces, and M.L. Espinas. 2020. Haspin kinase
930 modulates nuclear architecture and Polycomb-dependent gene silencing. *PLoS Genet*.
931 16:e1008962.
932 Funabiki, H. 2019. Correcting aberrant kinetochore microtubule attachments: a hidden regulation of
933 Aurora B on microtubules. *Curr Opin Cell Biol*. 58:34-41.
934 Gao, S., M.G. Giansanti, G.J. Buttrick, S. Ramasubramanyan, A. Auton, M. Gatti, and J.G. Wakefield.
935 2008. Australin: a chromosomal passenger protein required specifically for Drosophila
936 melanogaster male meiosis. *J Cell Biol*. 180:521-535.
937 Giauque, C.C., and S.E. Bickel. 2016. Heterochromatin-Associated Proteins HP1a and Piwi Collaborate to
938 Maintain the Association of Achiasmate Homologs in Drosophila Oocytes. *Genetics*. 203:173-
939 189.

940 Giet, R., and D.M. Glover. 2001. Drosophila aurora B kinase is required for histone H3 phosphorylation
941 and condensin recruitment during chromosome condensation and to organize the central
942 spindle during cytokinesis. *J Cell Biol*. 152:669-682.
943 Giunta, K.L., J.K. Jang, E.A. Manheim, G. Subramanian, and K.S. McKim. 2002. subito encodes a kinesin-
944 like protein required for meiotic spindle pole formation in Drosophila melanogaster. *Genetics*.
945 160:1489-1501.
946 Głuszek, A.A., C.F. Cullen, W. Li, R.A. Battaglia, S.J. Radford, M.F. Costa, K.S. McKim, G. Goshima, and H.
947 Ohkura. 2015. The microtubule catastrophe promoter Sentin delays stable kinetochore-
948 microtubule attachment in oocytes. *J Cell Biol*. 211:1113-1120.
949 Gohard, F.H., D.J. St-Cyr, M. Tyers, and W.C. Earnshaw. 2014. Targeting the INCENP IN-box-Aurora B
950 interaction to inhibit CPC activity in vivo. *Open Biol*. 4:140163.
951 Haase, J., M.K. Bonner, H. Halas, and A.E. Kelly. 2017. Distinct Roles of the Chromosomal Passenger
952 Complex in the Detection of and Response to Errors in Kinetochore-Microtubule Attachment.
953 *Dev Cell*. 42:640-654 e645.
954 Hadders, M.A., S. Hindriksen, M.A. Truong, A.N. Mhaskar, J.P. Wopken, M.J.M. Vromans, and S.M.A.
955 Lens. 2020. Untangling the contribution of Haspin and Bub1 to Aurora B function during mitosis.
956 *J Cell Biol*. 219.
957 Heald, R., and A. Khodjakov. 2015. Thirty years of search and capture: The complex simplicity of mitotic
958 spindle assembly. *J Cell Biol*. 211:1103-1111.
959 Heald, R., R. Tournebize, T. Blank, R. Sandaltzopoulos, P. Becker, A. Hyman, and E. Karsenti. 1996. Self-
960 organization of microtubules into bipolar spindles around artificial chromosomes in Xenopus egg
961 extracts. *Nature*. 382:420-425.
962 Heeger, S., O. Leismann, R. Schittenhelm, O. Schraidt, S. Heidmann, and C.F. Lehner. 2005. Genetic
963 interactions of separase regulatory subunits reveal the diverged Drosophila Cenp-C homolog.
964 *Genes Dev*. 19:2041-2053.
965 Hengeveld, R.C.C., M.J.M. Vromans, M. Vleugel, M.A. Hadders, and S.M.A. Lens. 2017. Inner centromere
966 localization of the CPC maintains centromere cohesion and allows mitotic checkpoint silencing.
967 *Nat Commun*. 8:15542.
968 Hindriksen, S., S.M.A. Lens, and M.A. Hadders. 2017. The Ins and Outs of Aurora B Inner Centromere
969 Localization. *Front Cell Dev Biol*. 5:112.
970 Hirota, T., J.J. Lipp, B.H. Toh, and J.M. Peters. 2005. Histone H3 serine 10 phosphorylation by Aurora B
971 causes HP1 dissociation from heterochromatin. *Nature*. 438:1176-1180.
972 Holubcová, Z., M. Blayney, K. Elder, and M. Schuh. 2015. Human oocytes. Error-prone chromosome-
973 mediated spindle assembly favors chromosome segregation defects in human oocytes. *Science*.
974 348:1143-1147.
975 Jang, J.K., T. Rahman, V.S. Kober, J. Cesario, and K.S. McKim. 2007. Misregulation of the Kinesin-like
976 Protein Subito Induces Meiotic Spindle Formation in the Absence of Chromosomes and
977 Centrosomes. *Genetics*. 177:267-280.
978 Jang, J.K., T. Rahman, and K.S. McKim. 2005. The kinesinlike protein Subito contributes to central spindle
979 assembly and organization of the meiotic spindle in Drosophila oocytes. *Mol Biol Cell*. 16:4684-
980 4694.
981 Jeyaprakash, A.A., U.R. Klein, D. Lindner, J. Ebert, E.A. Nigg, and E. Conti. 2007. Structure of a Survivin-
982 Borealin-INCENP core complex reveals how chromosomal passengers travel together. *Cell*.
983 131:271-285.
984 Kang, J., J. Chaudhary, H. Dong, S. Kim, C.A. Brautigam, and H. Yu. 2011. Mitotic centromeric targeting of
985 HP1 and its binding to Sgo1 are dispensable for sister-chromatid cohesion in human cells. *Mol
986 Biol Cell*. 22:1181-1190.

987 Karpen, G.H., M.H. Le, and H. Le. 1996. Centric heterochromatin and the efficiency of achiasmate
988 disjunction in Drosophila female meiosis. *Science*. 273:118-122.
989 Kelly, A.E., S.C. Sampath, T.A. Maniar, E.M. Woo, B.T. Chait, and H. Funabiki. 2007. Chromosomal
990 enrichment and activation of the aurora B pathway are coupled to spatially regulate spindle
991 assembly. *Dev Cell*. 12:31-43.
992 Klein, U.R., E.A. Nigg, and U. Gruneberg. 2006. Centromere targeting of the chromosomal passenger
993 complex requires a ternary subcomplex of Borealin, Survivin, and the N-terminal domain of
994 INCENP. *Mol Biol Cell*. 17:2547-2558.
995 Krenn, V., and A. Musacchio. 2015. The Aurora B Kinase in Chromosome Bi-Orientation and Spindle
996 Checkpoint Signaling. *Front Oncol*. 5:225.
997 Laband, K., R. Le Borgne, F. Edwards, M. Stefanutti, J.C. Canman, J.M. Verbavatz, and J. Dumont. 2017.
998 Chromosome segregation occurs by microtubule pushing in oocytes. *Nat Commun*. 8:1499.
999 Liu, D., G. Vader, M.J. Vromans, M.A. Lampson, and S.M. Lens. 2009. Sensing chromosome bi-orientation
1000 by spatial separation of aurora B kinase from kinetochore substrates. *Science*. 323:1350-1353.
1001 Liu, X., J. Shen, L. Xie, Z. Wei, C. Wong, Y. Li, X. Zheng, P. Li, and Y. Song. 2020. Mitotic Implantation of
1002 the Transcription Factor Prospero via Phase Separation Drives Terminal Neuronal
1003 Differentiation. *Dev Cell*. 52:277-293 e278.
1004 Liu, X., Z. Song, Y. Huo, J. Zhang, T. Zhu, J. Wang, X. Zhao, F. Aikhionbare, J. Zhang, H. Duan, J. Wu, Z.
1005 Dou, Y. Shi, and X. Yao. 2014. Chromatin protein HP1 interacts with the mitotic regulator
1006 borealin protein and specifies the centromere localization of the chromosomal passenger
1007 complex. *J Biol Chem*. 289:20638-20649.
1008 Maresca, T.J., A.C. Groen, J.C. Gatlin, R. Ohi, T.J. Mitchison, and E.D. Salmon. 2009. Spindle assembly in
1009 the absence of a RanGTP gradient requires localized CPC activity. *Curr Biol*. 19:1210-1215.
1010 Matthies, H.J., H.B. McDonald, L.S. Goldstein, and W.E. Theurkauf. 1996. Anastral meiotic spindle
1011 morphogenesis: role of the non-claret disjunctional kinesin-like protein. *J Cell Biol*. 134:455-464.
1012 Mullen, T.J., A.C. Davis-Roca, and S.M. Wignall. 2019. Spindle assembly and chromosome dynamics
1013 during oocyte meiosis. *Curr Opin Cell Biol*. 60:53-59.
1014 Muscat, C.C., K.M. Torre-Santiago, M.V. Tran, J.A. Powers, and S.M. Wignall. 2015. Kinetochore-
1015 independent chromosome segregation driven by lateral microtubule bundles. *eLife*. 4.
1016 Nicklas, R.B. 1997. How cells get the right chromosomes. *Science*. 275:632-637.
1017 Nozawa, R.S., K. Nagao, H.T. Masuda, O. Iwasaki, T. Hirota, N. Nozaki, H. Kimura, and C. Obuse. 2010.
1018 Human POGZ modulates dissociation of HP1alpha from mitotic chromosome arms through
1019 Aurora B activation. *Nat Cell Biol*. 12:719-727.
1020 Ohkura, H. 2015. Meiosis: an overview of key differences from mitosis. *Cold Spring Harbor perspectives*
1021 *in biology*. 7.
1022 Pamula, M.C., L. Carlini, S. Forth, P. Verma, S. Suresh, W.R. Legant, A. Khodjakov, E. Betzig, and T.M.
1023 Kapoor. 2019. High-resolution imaging reveals how the spindle midzone impacts chromosome
1024 movement. *J Cell Biol*. 218:2529-2544.
1025 Przewloka, M.R., W. Zhang, P. Costa, V. Archambault, P.P. D'Avino, K.S. Lilley, E.D. Laue, A.D. McAinsh,
1026 and D.M. Glover. 2007. Molecular analysis of core kinetochore composition and assembly in
1027 Drosophila melanogaster. *PloS one*. 2:e478.
1028 Radford, S.J., T.L. Hoang, A.A. Głuszek, H. Ohkura, and K.S. McKim. 2015. Lateral and End-On
1029 Kinetochore Attachments Are Coordinated to Achieve Bi-orientation in Drosophila Oocytes. *PLoS*
1030 *Genet*. 11:e1005605.
1031 Radford, S.J., J.K. Jang, and K.S. McKim. 2012. The Chromosomal Passenger Complex is required for
1032 Meiotic Acentrosomal Spindle Assembly and Chromosome Bi-orientation. *Genetics*. 192:417-
1033 429.

1034 Radford, S.J., and K.S. McKim. 2016. Techniques for Imaging Prometaphase and Metaphase of Meiosis I
1035 in Fixed Drosophila Oocytes. *J Vis Exp*. 116:e54666.
1036 Radford, S.J., A.L. Nguyen, K. Schindler, and K.S. McKim. 2017. The chromosomal basis of meiotic
1037 acentrosomal spindle assembly and function in oocytes. *Chromosoma*. 126:351-364.
1038 Reschen, R.F., N. Colombie, L. Wheatley, J. Dobbelaere, D. St Johnston, H. Ohkura, and J.W. Raff. 2012.
1039 Dgp71WD is required for the assembly of the acentrosomal Meiosis I spindle, and is not a
1040 general targeting factor for the gamma-TuRC. *Biol Open*. 1:422-429.
1041 Resnick, T.D., K.J. Dej, Y. Xiang, R.S. Hawley, C. Ahn, and T.L. Orr-Weaver. 2009. Mutations in the
1042 chromosomal passenger complex and the condensin complex differentially affect synaptonemal
1043 complex disassembly and metaphase I configuration in Drosophila female meiosis. *Genetics*.
1044 181:875-887.
1045 Rome, P., and H. Ohkura. 2018. A novel microtubule nucleation pathway for meiotic spindle assembly in
1046 oocytes. *J Cell Biol*. 217:3431-3445.
1047 Rorth, P., K. Szabo, A. Bailey, T. Laverty, J. Rehm, G.M. Rubin, K. Weigmann, M. Milan, V. Benes, W.
1048 Ansorge, and S.M. Cohen. 1998. Systematic Gain-of-Function Genetics in Drosophila.
1049 *Development*. 125:1049-1057.
1050 Ruppert, J.G., K. Samejima, M. Platani, O. Molina, H. Kimura, A.A. Jeyaprakash, S. Ohta, and W.C.
1051 Earnshaw. 2018. HP1alpha targets the chromosomal passenger complex for activation at
1052 heterochromatin before mitotic entry. *EMBO J*. 37.
1053 Salimian, K.J., E.R. Ballister, E.M. Smoak, S. Wood, T. Panchenko, M.A. Lampson, and B.E. Black. 2011.
1054 Feedback control in sensing chromosome biorientation by the Aurora B kinase. *Curr Biol*.
1055 21:1158-1165.
1056 Samejima, K., M. Platani, M. Wolny, H. Ogawa, G. Vargiu, P.J. Knight, M. Peckham, and W.C. Earnshaw.
1057 2015. The Inner Centromere Protein (INCENP) Coil Is a Single alpha-Helix (SAH) Domain That
1058 Binds Directly to Microtubules and Is Important for Chromosome Passenger Complex (CPC)
1059 Localization and Function in Mitosis. *J Biol Chem*. 290:21460-21472.
1060 Sampath, S.C., R. Ohi, O. Leismann, A. Salic, A. Pozniakovski, and H. Funabiki. 2004. The chromosomal
1061 passenger complex is required for chromatin-induced microtubule stabilization and spindle
1062 assembly. *Cell*. 118:187-202.
1063 Schittenhelm, R.B., S. Heeger, F. Althoff, A. Walter, S. Heidmann, K. Mechtler, and C.F. Lehner. 2007.
1064 Spatial organization of a ubiquitous eukaryotic kinetochore protein network in Drosophila
1065 chromosomes. *Chromosoma*. 116:385-402.
1066 Schuh, M., and J. Ellenberg. 2007. Self-organization of MTOCs replaces centrosome function during
1067 acentrosomal spindle assembly in live mouse oocytes. *Cell*. 130:484-498.
1068 Serena, M., R.N. Bastos, P.R. Elliott, and F.A. Barr. 2020. Molecular basis of MKLP2-dependent Aurora B
1069 transport from chromatin to the anaphase central spindle. *J Cell Biol*. 219.
1070 Simunic, J., and I.M. Tolic. 2016. Mitotic Spindle Assembly: Building the Bridge between Sister K-Fibers.
1071 *Trends Biochem Sci*. 41:824-833.
1072 Smurnyy, Y., A.V. Toms, G.R. Hickson, M.J. Eck, and U.S. Eggert. 2010. Binucleine 2, an isoform-specific
1073 inhibitor of Drosophila Aurora B kinase, provides insights into the mechanism of cytokinesis. *ACS*
1074 *Chem Biol*. 5:1015-1020.
1075 So, C., K.B. Seres, A.M. Steyer, E. Monnich, D. Clift, A. Pejkovska, W. Mobius, and M. Schuh. 2019. A
1076 liquid-like spindle domain promotes acentrosomal spindle assembly in mammalian oocytes.
1077 *Science*. 364.
1078 Sugimura, I., and M.A. Lilly. 2006. Bruno inhibits the expression of mitotic cyclins during the prophase I
1079 meiotic arrest of Drosophila oocytes. *Dev Cell*. 10:127-135.
1080 Szafer-Glusman, E., M.T. Fuller, and M.G. Giansanti. 2011. Role of Survivin in cytokinesis revealed by a
1081 separation-of-function allele. *Mol Biol Cell*. 22:3779-3790.

1082 Tanaka, T.U., N. Rachidi, C. Janke, G. Pereira, M. Galova, E. Schiebel, M.J. Stark, and K. Nasmyth. 2002.
1083 Evidence that the Ipl1-Sli15 (Aurora kinase-INCENP) complex promotes chromosome bi-
1084 orientation by altering kinetochore-spindle pole connections. *Cell*. 108:317-329.
1085 Theurkauf, W.E., and R.S. Hawley. 1992. Meiotic spindle assembly in Drosophila females: behavior of
1086 nonexchange chromosomes and the effects of mutations in the nod kinesin-like protein. *J Cell*
1087 *Biol*. 116:1167-1180.
1088 Trivedi, P., F. Palomba, E. Niedzialkowska, M.A. Digman, E. Gratton, and P.T. Stukenberg. 2019a. The
1089 inner centromere is a biomolecular condensate scaffolded by the chromosomal passenger
1090 complex. *Nat Cell Biol*. 21:1127-1137.
1091 Trivedi, P., and P.T. Stukenberg. 2020. A Condensed View of the Chromosome Passenger Complex.
1092 *Trends Cell Biol*.
1093 Trivedi, P., A.V. Zaytsev, M. Godzi, F.I. Ataullakhanov, E.L. Grishchuk, and P.T. Stukenberg. 2019b. The
1094 binding of Borealin to microtubules underlies a tension independent kinetochore-microtubule
1095 error correction pathway. *Nat Commun*. 10:682.
1096 Tseng, B.S., L. Tan, T.M. Kapoor, and H. Funabiki. 2010. Dual Detection of Chromosomes and
1097 Microtubules by the Chromosomal Passenger Complex Drives Spindle Assembly. *Dev Cell*.
1098 18:903-912.
1099 van der Horst, A., and S.M. Lens. 2014. Cell division: control of the chromosomal passenger complex in
1100 time and space. *Chromosoma*. 123:25-42.
1101 van der Horst, A., M.J. Vromans, K. Bouwman, M.S. van der Waal, M.A. Hadders, and S.M. Lens. 2015.
1102 Inter-domain Cooperation in INCENP Promotes Aurora B Relocation from Centromeres to
1103 Microtubules. *Cell reports*. 12:380-387.
1104 Venkei, Z., M.R. Przewloka, Y. Ladak, S. Albadri, A. Sossick, G. Juhasz, B. Novak, and D.M. Glover. 2012.
1105 Spatiotemporal dynamics of Spc105 regulates the assembly of the Drosophila kinetochore. *Open*
1106 *Biol*. 2:110032.
1107 Vukusic, K., R. Buda, A. Bosilj, A. Milas, N. Pavin, and I.M. Tolic. 2017. Microtubule Sliding within the
1108 Bridging Fiber Pushes Kinetochore Fibers Apart to Segregate Chromosomes. *Dev Cell*. 43:11-23
1109 e16.
1110 Wang, F., J. Dai, J.R. Daum, E. Niedzialkowska, B. Banerjee, P.T. Stukenberg, G.J. Gorbsky, and J.M.
1111 Higgins. 2010. Histone H3 Thr-3 phosphorylation by Haspin positions Aurora B at centromeres in
1112 mitosis. *Science*. 330:231-235.
1113 Wang, L.I., A. Das, and K.S. McKim. 2019. Sister centromere fusion during meiosis I depends on
1114 maintaining cohesins and destabilizing microtubule attachments. *PLoS Genet*. 15:e1008072.
1115 Watanabe, Y. 2012. Geometry and force behind kinetochore orientation: lessons from meiosis. *Nat Rev*
1116 *Mol Cell Biol*. 13:370-382.
1117 Wheelock, M.S., D.J. Wynne, B.S. Tseng, and H. Funabiki. 2017. Dual recognition of chromatin and
1118 microtubules by INCENP is important for mitotic progression. *J Cell Biol*. 216:925-941.
1119 Wignall, S.M., and A.M. Villeneuve. 2009. Lateral microtubule bundles promote chromosome alignment
1120 during acentrosomal oocyte meiosis. *Nat Cell Biol*. 11:839-844.
1121 Williams, M.M., A.J. Mathison, T. Christensen, P.T. Greipp, D.L. Knutson, E.W. Klee, M.T. Zimmermann, J.
1122 Iovanna, G.A. Lomberk, and R.A. Urrutia. 2019. Aurora kinase B-phosphorylated HP1alpha
1123 functions in chromosomal instability. *Cell Cycle*. 18:1407-1421.
1124 Wu, C., V. Singaram, and K.S. McKim. 2008. mei-38 is required for chromosome segregation during
1125 meiosis in Drosophila females. *Genetics*. 180:61-72.
1126 Xu, Z., H. Ogawa, P. Vagnarelli, J.H. Bergmann, D.F. Hudson, S. Ruchaud, T. Fukagawa, W.C. Earnshaw,
1127 and K. Samejima. 2009. INCENP-aurora B interactions modulate kinase activity and chromosome
1128 passenger complex localization. *J Cell Biol*. 187:637-653.

1129 Yamagishi, Y., T. Honda, Y. Tanno, and Y. Watanabe. 2010. Two histone marks establish the inner
1130 centromere and chromosome bi-orientation. *Science*. 330:239-243.

1131

1132 Figure 1

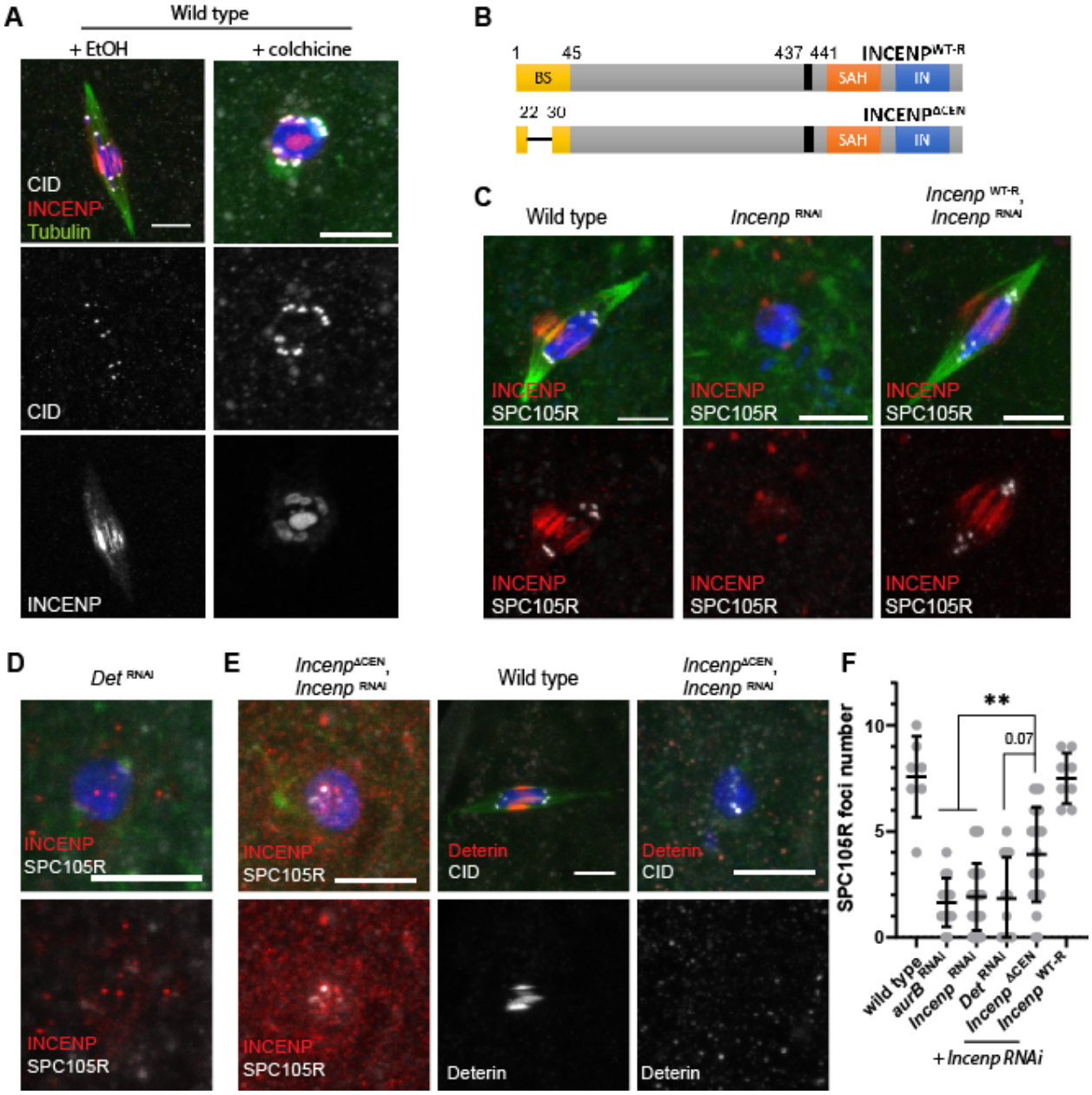

1133

1134 Figure 2

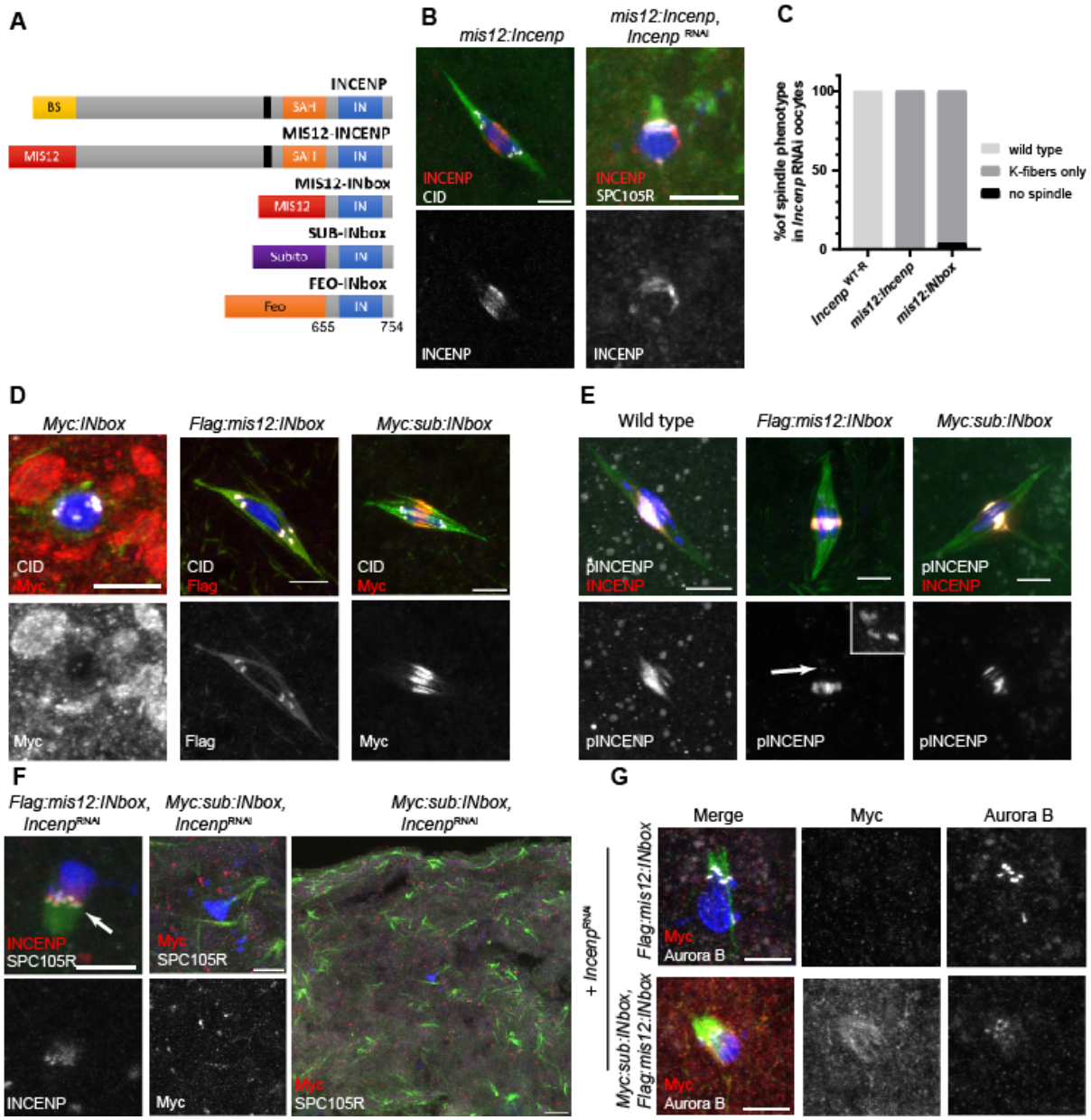

1135

1136 Figure 3

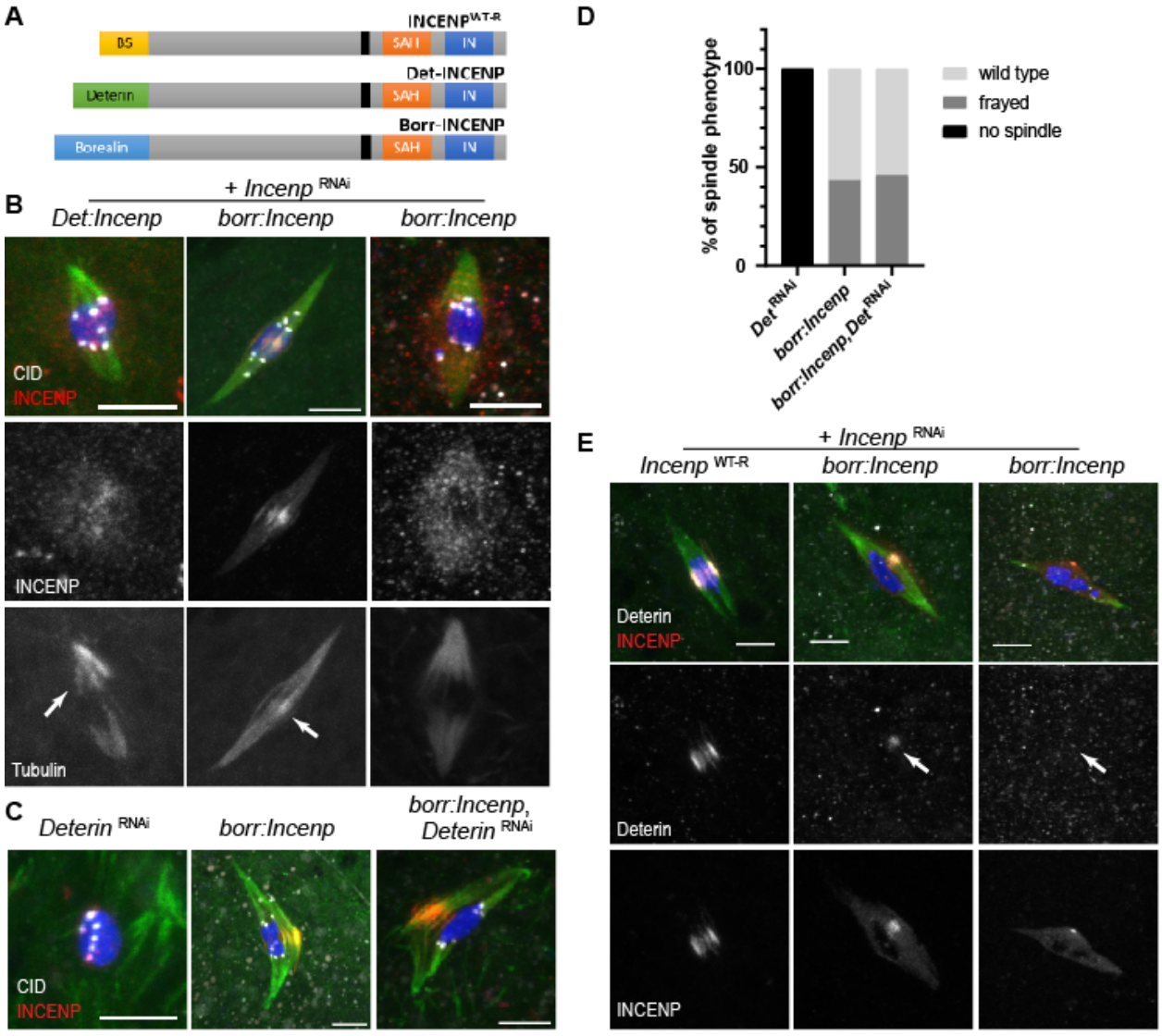

1137

Figure 4

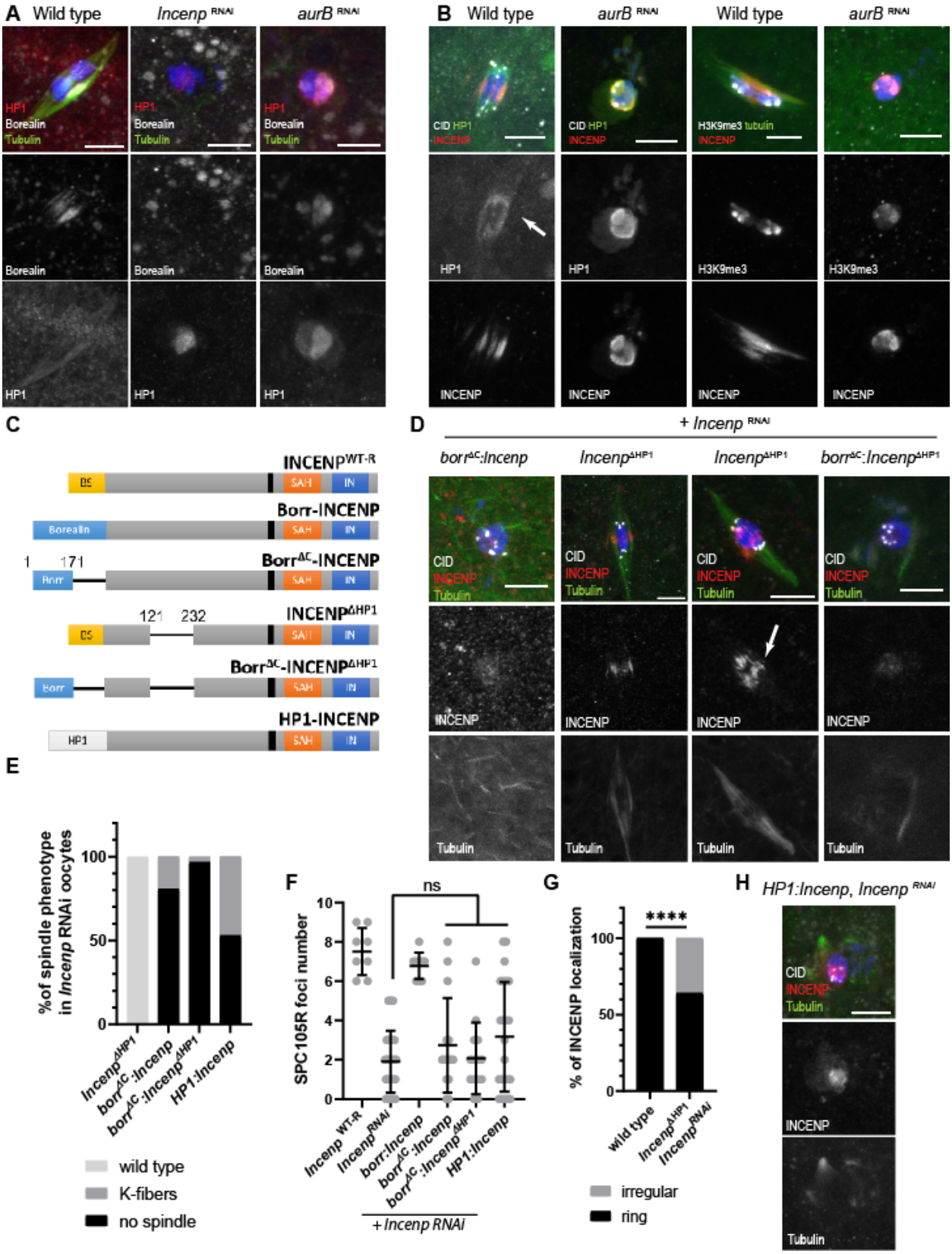
A
Wild type
Incenp RNAi
aurB RNAi
HP1
Borealin
Tubulin
B
Wild type
aurB RNAi
Wild type
aurB RNAi
CID HP1
INCENP
H3K9me3 tubulin
INCENP
HP1
H3K9me3
INCENP
C
INCENPWT-R
Borr-INCENP
BorrΔC-INCENP
INCENPΔHP1
BorrΔC-INCENPΔHP1
HP1-INCENP
1
171
121
232
D
+ Incenp RNAi
borrΔC:Incenp
IncenpΔHP1
IncenpΔHP1
borrΔC:IncenpΔHP1
CID
INCENP
Tubulin
E
%of spindle phenotype in Incenp RNAi oocytes
100
50
0
IncenpΔHP1
borrΔC:Incenp
borrΔC:IncenpΔHP1
HP1:Incenp
wild type
K-fibers
no spindle
F
SPC105R foci number
ns
10
8
6
4
2
0
IncenpWT-R
IncenpRNAi
borr:Incenp
borrΔC:Incenp
borrΔC:IncenpΔHP1
HP1:Incenp
+ Incenp RNAi
G
% of INCENP localization
****
100
50
0
wild type
IncenpΔHP1
IncenpRNAi
irregular
ring
H
HP1:Incenp, Incenp RNAi
CID
INCENP
Tubulin
INCENP
Tubulin

1140 Figure 5

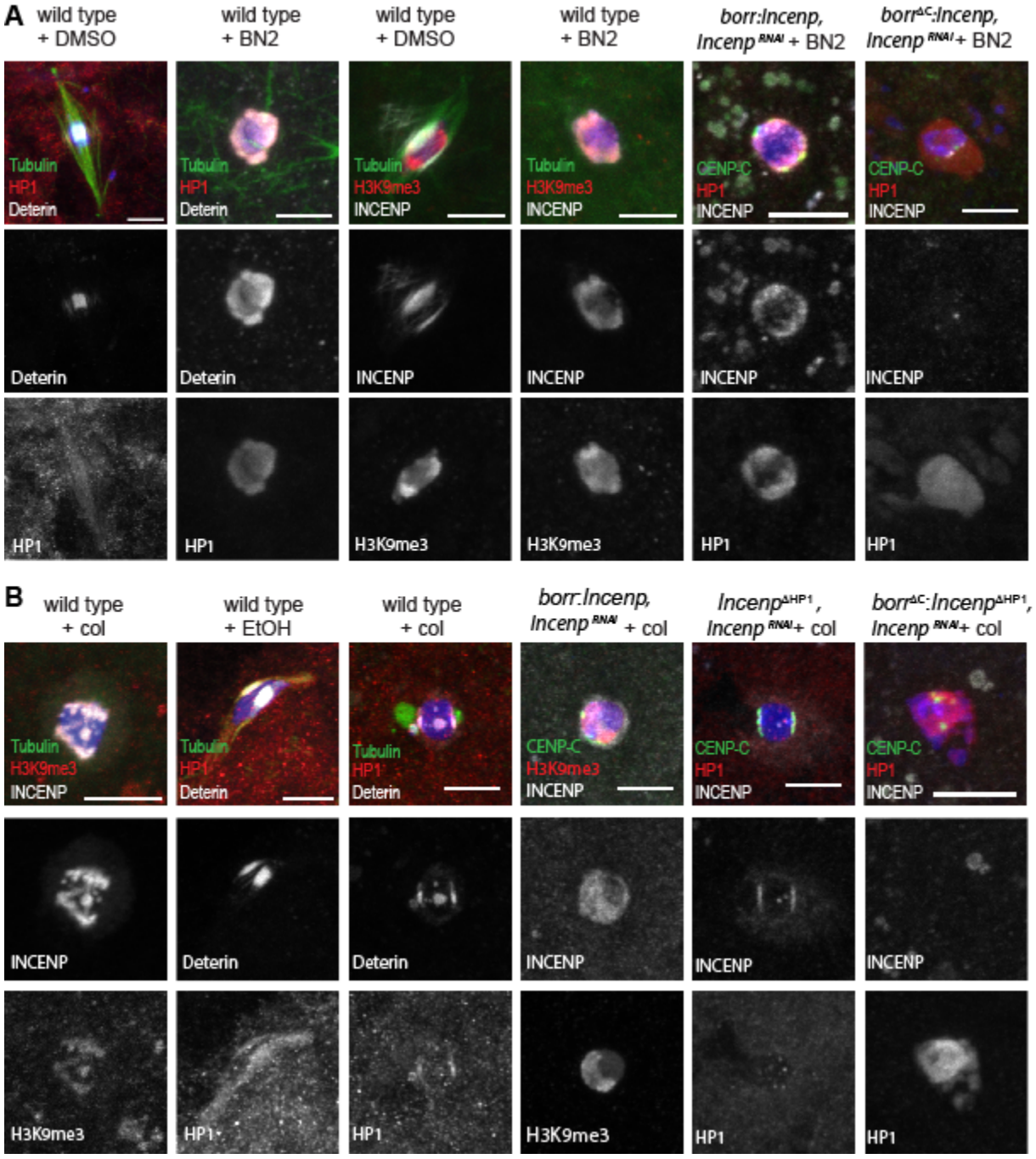

1141

1142 Figure 6

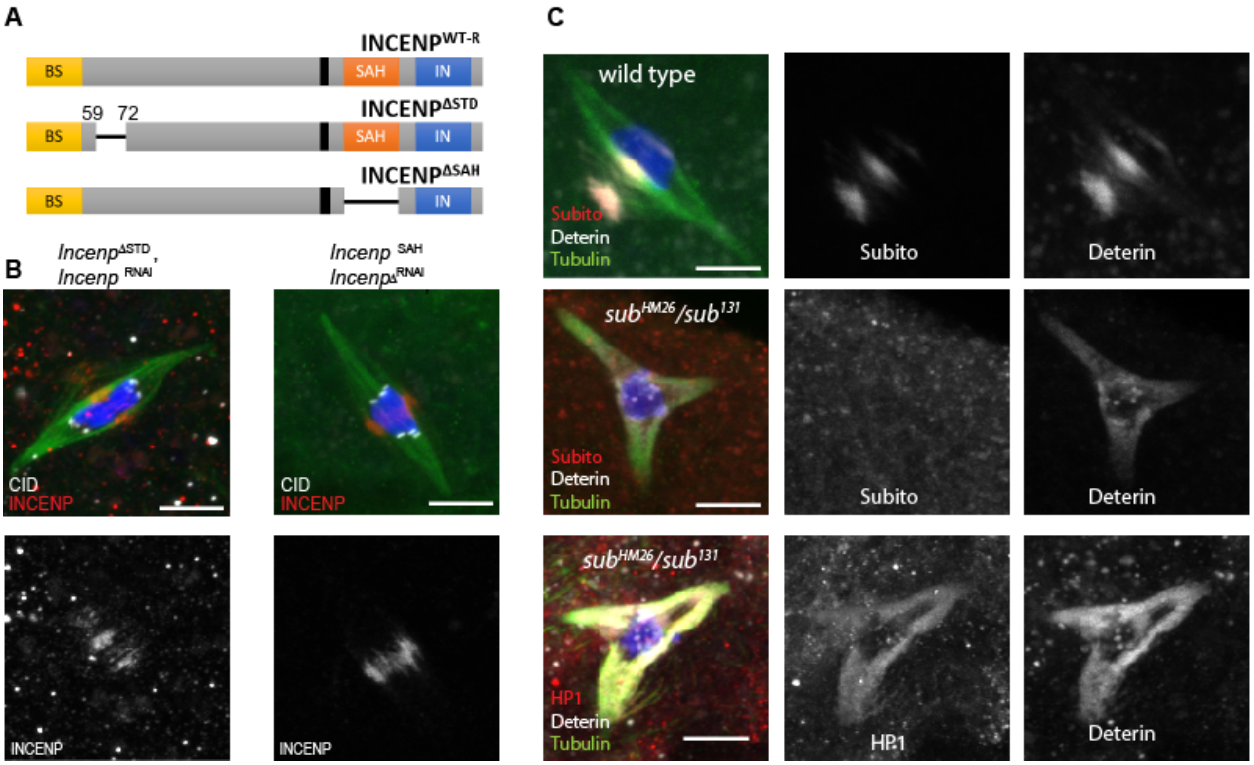

1143

1144 Figure 7

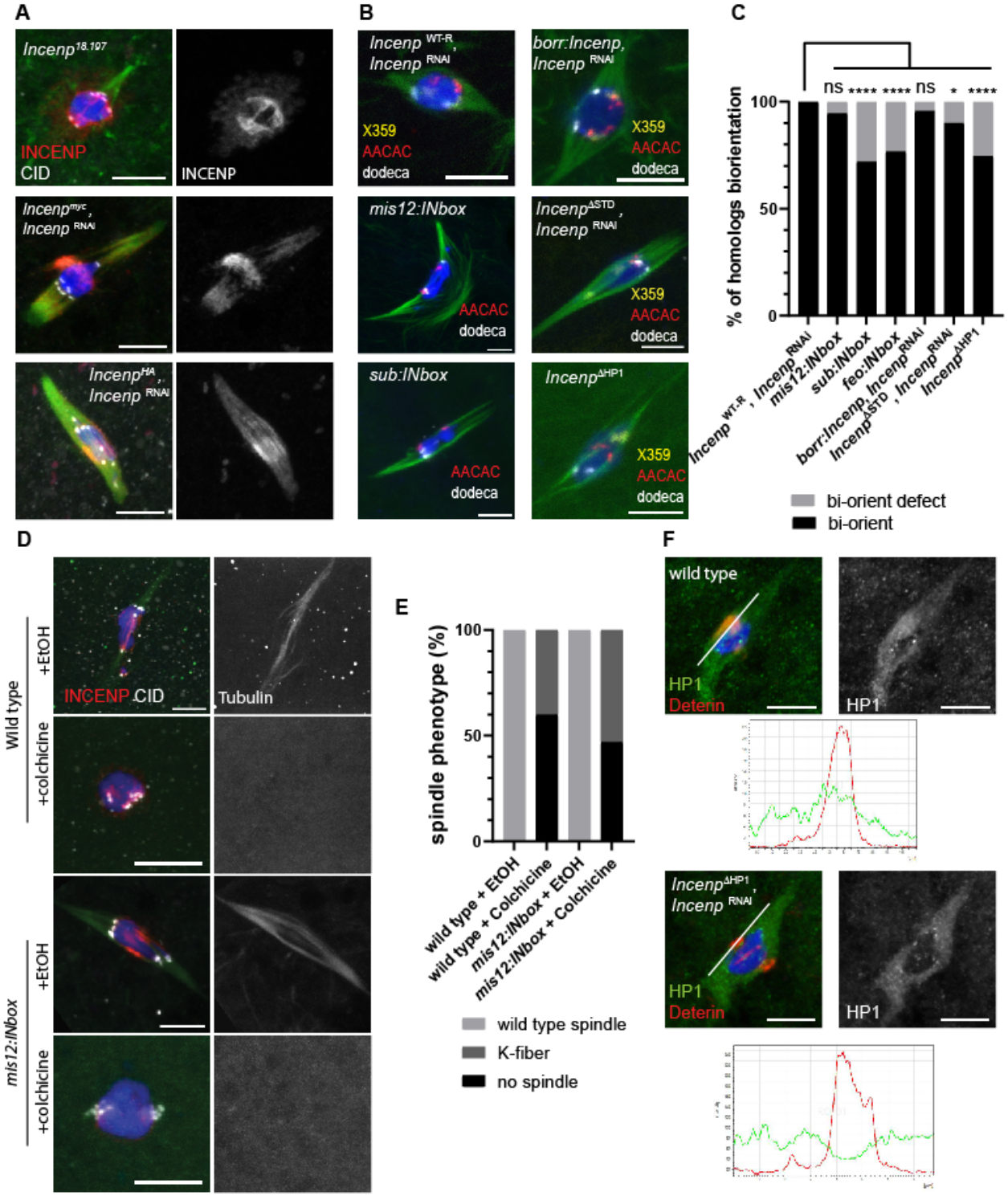

1145

1146 Figure 8

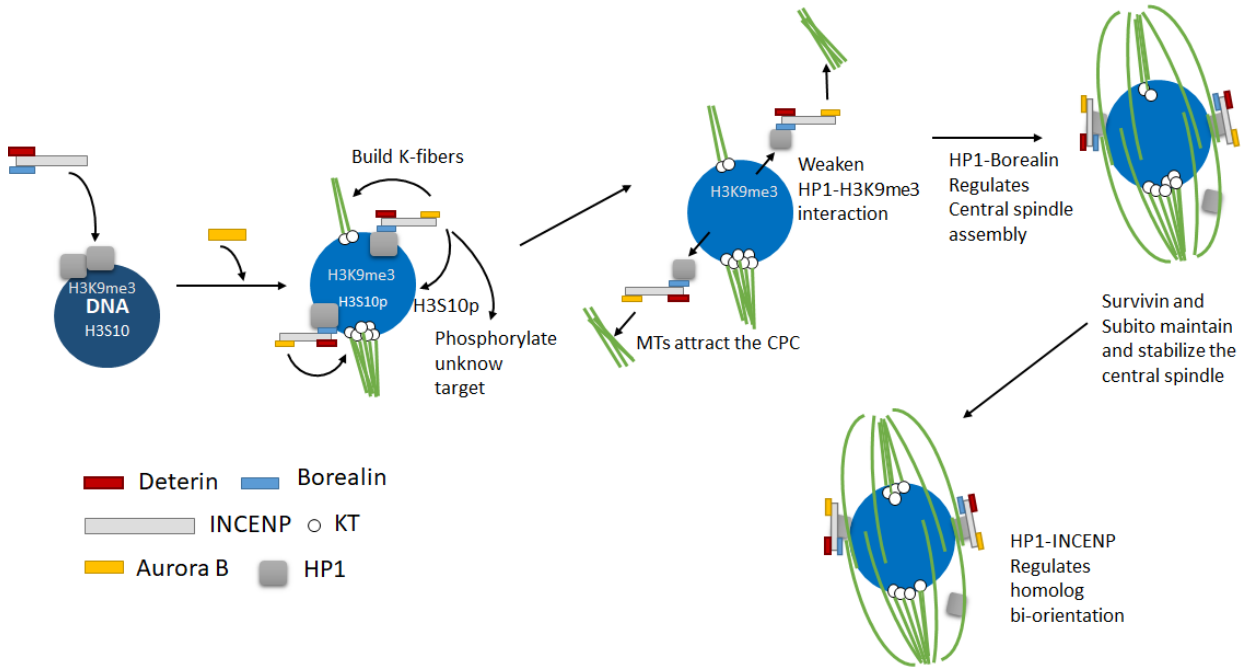

1147

1148